JOURNAL OF APPLIED PHYSICS

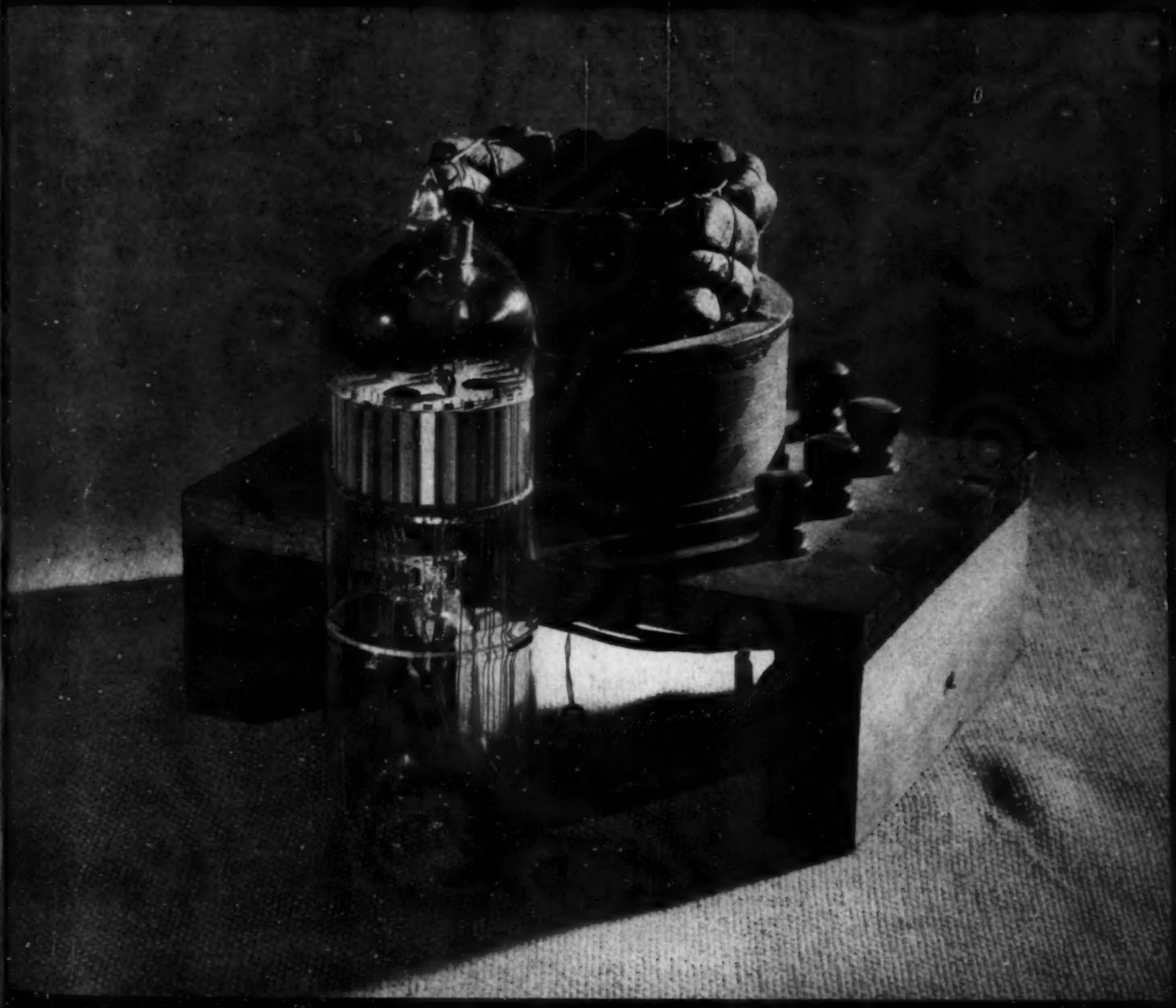

JOURNAL OF APPLIED PHYSICS

Vol. 15, No. 10 OCTOBER, 1944

In This Issue

Page

Historical Background of Electron Optics C. J. CALBICK 685

Electron Microscope in Metallurgical Research CHARLES S. BARRETT 691

Extending Microscopic Examination of Metals F. KELLER AND A. H. GEISLER 696

Magnetically Focused Radial Beam Vacuum Tube A. M. SKELLETT 704

Kinematics of Reflection Oscillators A. E. HARRISON 709

Thickness of Electron Microscopic Objects ROBLEY C. WILLIAMS AND RALPH W. G. WYCKOFF 712

Potential Nuclear Monokinetic Electron Sources M. L. POOL 716

Contributed Original Research

Limiting Stable Current in Electron Beams in the Presence of Ions J. R. PIERCE 721

Letter to the Editor

Stereoscopy with the Electron Microscope L. MARTON 726

In Every Issue

Here and There 718

New Book 720

Calendar of Meetings 727

Recent Applications of Physics 728

Index to Advertisers xxviii

BOARD OF EDITORS

ELMER HUTCHISSON, *Editor*

Associate Editors

R. B. BARNES
OTTO BEECK
W. F. BUSSE
S. H. CALDWELL
CLARK GOODMAN
SELIG HECHT
W. J. LYONS
MORRIS MUSKAT
THOMAS H. OSGOOD
PAUL E. SABINE
FREDERICK SEITZ
J. R TOWNSEND

Publication of the American Institute of Physics

ADMINISTRATIVE STAFF

HENRY A. BARTON, *Director*

MADELINE M. MITCHELL, *Publications Manager*

JOHN T. TATE, *Adviser on Publications*

GOVERNING BOARD

PAUL E. KLOPSTEG, *Chairman*

GEORGE B. PEGRAM, *Secretary*

T. D. COPE
R. B. DOW
L. A. DUBRIDGE
FLOYD A. FIRESTONE
HARVEY FLETCHER
R. C. GIBBS
K. S. GIBSON
HERMANN MARK
A. G. WORTHING
JOHN T. TATE
L. W. TAYLOR
N. W. TAYLOR
WALLACE WATERFALL

The JOURNAL OF APPLIED PHYSICS, published monthly at Prince and Lemon Sts., Lancaster, Pa., is devoted to physics in its role as the science basic to other natural sciences and to the arts and industries. Previous to 1937 this publication was known as PHYSICS. The JOURNAL OF APPLIED PHYSICS publishes editorials, news of physicists, and reviews, as well as technical papers of applied physics.

Manuscripts should be submitted to Elmer Hutchisson, Editor, 50th floor, 350 Fifth Avenue, New York 1, New York.

Subscriptions and orders for back numbers should be addressed to Prince and Lemon Streets, Lancaster, Pa. or to the American Institute of Physics, 57 East 55 Street, New York 22, N. Y.

Subscription Price

	U. S. AND CANADA	ELSEWHERE
To members of scientific societies	$5.00	$5.70
To all others	7.00	7.70

Back Number Prices

Complete set: Vol. 1, July, 1931–Vol. 14, 1943—**$87.50**
Yearly back number rate: **$7.70**
Single copies: **$0.70** each.

Changes of address and proofs should be addressed to the Publications Manager.

Advertising rates supplied on request. Orders, advertising copy, and cuts should be sent to the American Institute of Physics.

Entered as second class matter January 22, 1937, at the Post Office at Lancaster, Pennsylvania, under the Act of March 3, 1879
Accepted for mailing at the special rate of postage provided for in the Act of February 28, 1925, authorized May 2, 1932.

Copyright 1944, by the American Institute of Physics.

The JOURNAL OF APPLIED PHYSICS is faced with serious difficulties because of the increasing volume of material submitted for publication and the decreasing supply of paper available under present WPB restrictions. As a partial solution to these difficulties, beginning with this issue and continuing as long as necessary, the Journal will use a lighter weight paper than formerly. Cooperation of contributors in reporting their work concisely and in remaining patient with a longer printing schedule will be greatly appreciated. —The Editor.

Journal of Applied Physics

Volume 15, Number 10 · **October, 1944**

Historical Background of Electron Optics*

BY C. J. CALBICK

Bell Telephone Laboratories, Inc., New York, New York

AMONG physical theories there are some which because of the great weight of experimental evidence have become laws rather than theories. Such is the case for the laws governing the interaction of free charged particles and electric and magnetic fields. It was in the attempt to apply these laws to certain very practical scientific and engineering problems that electron optics was born.

Less than 15 years ago, the art of producing beams of charged particles was in what might be called the pinhole camera stage. A physicist desiring to produce a narrow beam of electrons designed an electron gun consisting of a series of aligned holes (Fig. 1). He mounted a thermionic source K such as a tungsten or oxide-coated wire or ribbon filament. In front he mounted a box consisting of a series of aligned holes and behind it he might place a disk, possibly cup-shaped, which might be insulated from the cathode; or he might place between K and P an insulated disk to be operated at an intermediate potential. To investigate the beam produced by such a gun, he would design a collector, illustrated in the slide by three boxes, one inside the other insulated from each other. The first of these would be operated at the same potential as the anode of the gun, the second as a shield box at the same potential as the inner or collector box. With guns and collectors such as these the original Davisson and Germer electron diffraction[1] and reflection[2] experiments were made. We then investigated the possibility of electron polarization by a double-reflection[3] experiment. The result was indeterminate, and it was evident that the divergence of the electron beam and lack of resolving power in the collector were the limiting factors.

Now let us go back quite a bit. Some of the very early experiments on cathode rays by Sir William Crookes employed an apertured disk, the source of electrons being a glow discharge. Because of the very imperfect vacuum, gas focusing of the beam occurred, and the luminous

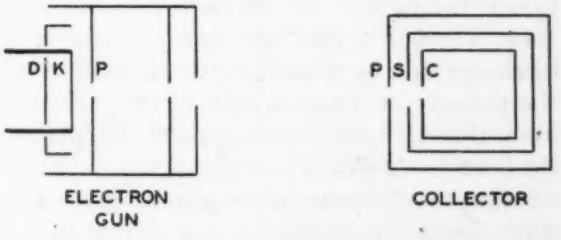

FIG. 1. Early form of electron gun to produce a narrow beam of electrons.

* Paper presented at the inaugural meeting of the Division of Electron and Ion Optics of the American Physical Society at Pittsburgh on April 29, 1944.

pencils of cathode rays struck the glass of the tube and excited fluorescence. They could be deflected by electric and magnetic fields and thus were found to carry a negative charge. They were christened electrons by Johnstone Stoney about the time (1897) that J. J. Thomson[4] designed the tube shown in Fig. 2 to measure e/m.

In the same year, Braun[5] developed the first cathode-ray oscillograph tube, which had been suggested by Hess in 1894. It is also shown in

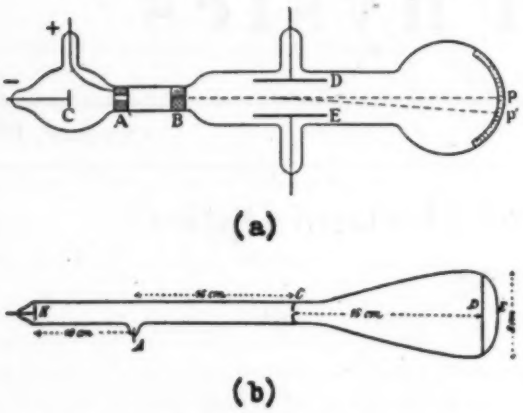

FIG. 2. (a) Tube for measuring e/m used by J. J. Thompson in 1897. (b) First cathode-ray oscillograph.

Fig. 2. In these tubes, gas focusing occurred and the beams remained of fairly small cross section out to the fluorescent screen.

It was early discovered that axial magnetic fields, either solenoidal or short, had a concentrating effect on the electron beam. During the next 30 years, the Braun tube was vastly improved. Improvements in vacuum technique led to the development of continuously pumped tubes in which the pressure in the deflection space was kept quite low and the electron beam was concentrated by magnetic means. Figure 3 shows the essential elements of a Braun tube. Usually the whole structure is at earth potential except the cathode at the end of the discharge tube. Through a leak tube the pressure in the discharge tube is maintained at about 10^{-2} mm, the pressure in the remainder of the tube being lower than 10^{-4} mm. A pair of deflecting plates in the beam withholding chamber serves to prevent damage to screen or photographic plate by a static beam. Concentrating coil, bias coils, and deflecting coils complete the oscillograph tube.

In 1926 and 1927, Busch,[6] in the Physical Institute in Jena, made a theoretical analysis of the action of concentrating coils in which he developed the fundamental formulae of magnetic electron optics. He subjected these formulae to experimental check finding very good agreement between experiment and theory. The differential equation of the trajectory of an electron developed by Busch is a lens equation, that is, it has the property that the angular change in direction of motion is proportional to the displacement from the axis. If the electrons form a beam with a definite convergence at any z plane, they will remain a beam at all z planes. Axially symmetric electric and magnetic fields, therefore, constitute lenses for electrons. Busch was primarily interested in magnetic focusing of beams in Braun tubes, and did not develop formulae for electrostatic lenses, although it is, of course, implicit in his equation that the second derivative of the electrostatic potential has a focusing effect similar to that of a magnetic field.

At this point, I should like to digress briefly for a discussion of the low voltage, gas-focused oscillograph tube developed about 1920 by Dr. J. B. Johnson[7] in the Bell Telephone Laboratories, then the Engineering Department of the Western Electric Company (Fig. 4). A spiral cathode C, either tungsten or oxide coated, was enclosed in an internal glass tube within which was mounted a disk D and a hollow cylindrical anode A. The purpose of the internal glass tube was to prevent excess bombardment of the cathode by ions

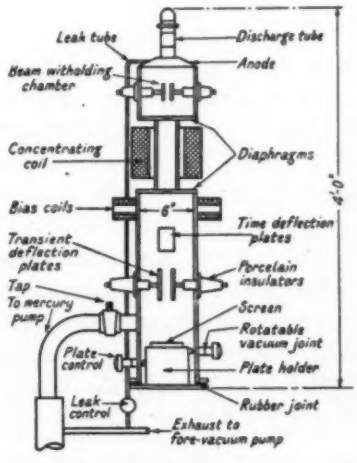

FIG. 3. The oscillograph of Miller and Robinson.

leaking around the sides of the disk *D*. Ions traveling backward along the electron beam passed down the center of the spiral so the cathode was not subjected to excessive bombardment. The structure shown was then mounted inside a glass envelope of the usual type for low voltage oscillographs. It was pumped to a carefully controlled pressure of a noble gas such as argon and sealed off. In terms of electron optics the focal power per unit length of the ion column depends on the density of the ions and the energy of the electrons. The density of the ions is roughly proportional to the beam current. Focusing was usually accomplished by varying the beam current, electrode potentials being fixed. Similar tubes were developed by laboratories in other countries. Because they operated at low voltages, they were in extensive use in the study of electric phenomena in the latter part of the 1920's. With such tubes, if the focal power were a little less than necessary for production of the smallest spot, a small circle of fluorescence was observed upon the screen. Dr. Johnson believed this to be an image of the spiral cathode, and we now recognize it as having been an electron micrograph of the filament as seen in its own emission. Because the focal power was uniformly distributed along the beam, the magnification was not large. It could, of course, be varied by varying the relative potentials of the disk *D* and anode *A*.

Now to return to the development of electron optics in Germany. The application of electron optics to the high voltage oscilloscope was pursued energetically, resulting in a much improved oscilloscope described by Knoll and Ruska in 1931. In two papers[8] in the *Annalen der Physik* in early 1932, Knoll and Ruska foreshadowed the invention of the electron microscope in their discussion of ray trajectories in cold cathode tubes and also presented certain forms of electrical lenses. These consist of metallic gauze assemblies resembling ordinary light lenses in their contours. In these papers electron micrographs of apertures

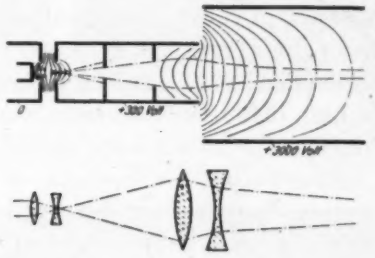

FIG. 6. Electron-optical parts of an early high vacuum cathode-ray oscilloscope (Zworykin).

illuminated by electrons made both by the electric and the magnetic lenses are exhibited. The title of these papers is "Contribution to geometrical electron optics"—the first time that the term electron optics occurs in the title of an article—although Busch, in his analysis, clearly delineated the analogy between magnetic lenses and light optics.

Shortly afterward, Brüche and Johannson[9] published the first paper on the electron microscope (May, 1932). Figure 5 shows the first electron micrograph of an emitting surface, taken from that paper. In 1933, Scherzer[10] published a general analysis of electrostatic lenses. In 1934, Johannson[11] described several forms of electrostatic electron microscopes, and Brüche and Scherzer published a monograph on geometrical electron optics, which includes a very complete bibliography of work done up to that time.

Before proceeding with a brief description of the electron lens experiments of Davisson and Calbick, I should like to mention the work of some other investigators. In 1913, Coolidge placed a cup-shaped electrode around a tungsten filament to focus the electrons into a small spot upon the anode used for the generation of x-rays. In 1923, A. B. Wood in England suggested this

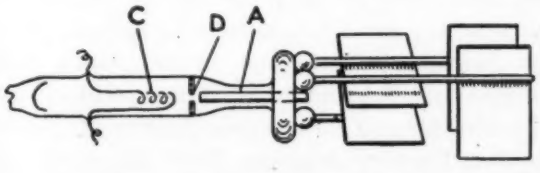

FIG. 4. Diagram of electron gun.

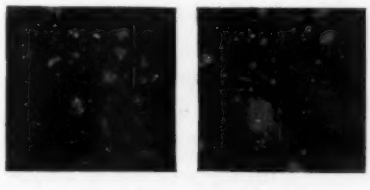

FIG. 5. First electron micrograph made with 300-volt electrons (Brüche and Johannson).

method might be used to obtain a good beam in a hot cathode oscilloscope. In 1927, E. E. Watson[12] published an article entitled "On the dispersion of electron beams." It is possible to extend his analysis and obtain electron-optical expressions. In 1931 Zworykin[13] described an improved high vacuum cathode-ray oscilloscope. Since then, he and his collaborators have developed the electrostatically focused cathode-ray tube to a high degree of perfection, described in Maloff and Epstein's book *Electron Optics in Television*. Figure 6 shows the electron-optical parts of an early tube of this type.

Under the stimulus of a search for a practical system of high definition television, many laboratories during the 1930's were simultaneously pushing forward the development of applied electron optics. Zworykin's iconoscope presented the problem of an oblique incident surface; Farnsworth's image dissector tube required deflection of a whole picture across an aperture, electrostatic electron multipliers required a succession of image surfaces so arranged that electrons emitted by one surface were concentrated into a smaller area on the next surface. In most cases, the fields were not calculable, so empirical methods of field and trajectory determination were developed—probe methods, the electrolytic trough, and the stretched rubber diaphragm, to mention three.

Aberrations of electron-optical images were from the first the subject of theoretical and experimental investigation. The electrons always exhibited a distribution in velocity, so chromatic aberration occurred. Most of the lenses used had relatively wide angular apertures, so spherical aberration and coma also occurred. Also, perfect

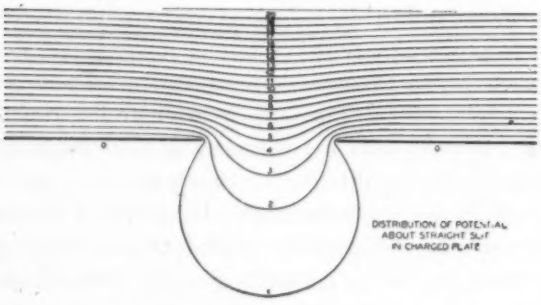

FIG. 7. Distribution of potential on a straight slit on a charged plate.

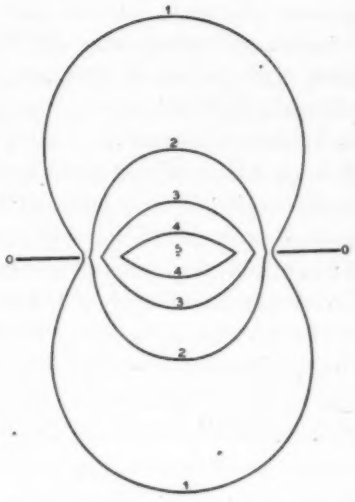

FIG. 8. Electrostatic field distortion due to straight slit in charged plate.

axial symmetry seldom was obtained, so astigmatism was a common fault. Deflecting plates were found to be essentially astigmatic, the optical analogy being that of a combined prism and cylindrical lens. Just as in light optics, however, it is the study and correction of aberrations which have led to the very considerable advances that have since been made in electron optics. Practically every electron-optical investigator has encountered the problems of aberration, and made contributions to their solution. I shall mention only a few of the investigators: Rogowski in Germany, Maloff and Epstein, and in later years, Ramberg and Spangenburg in this country. Of course, much of the finest work on aberration has been done in the perfecting of the electron microscope, and I would need to call the roll of the leading investigators in this field, from Bruche and Johannsen to Marton, Hillier, and the other present leaders, practically all of whom, in one form or another, have advanced our knowledge of the aberrations of electron lenses.

In the latter part of 1929, Dr. Davisson and I started a theoretical and experimental investigation whose object was to obtain really good electron guns and collectors. The simple case of the field about a slit in a charged plate was amenable to calculations and is shown in Fig. 7 for the case of a uniform gradient on one side and a field-free space on the other. If from this field we subtract the field that would exist if the slit

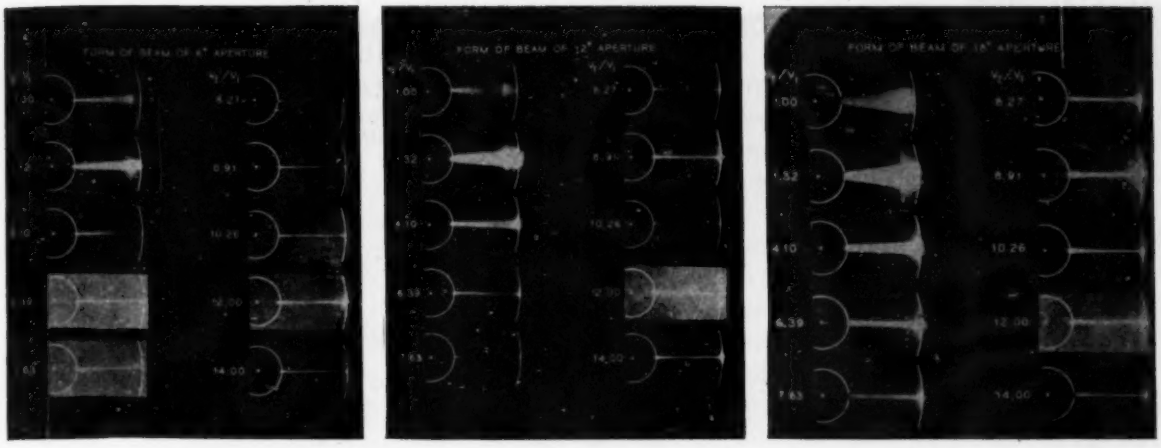

FIG. 9. Photographs of electron trajectories in a tube containing a pressure of mercury vapor so low that ionic space charge effects are negligible (cylindrical lenses in concentric cylinders).

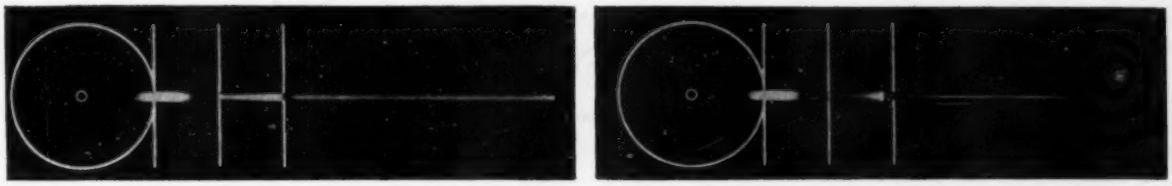

FIG. 10. Similar to Fig. 9 except tubes with plates containing circular apertures were used.

were not there, the field shown in Fig. 8 is obtained. The shape of the lines is suggestive of a lens, of course. The trajectory of an electron traversing such a field can be calculated and it is found that its angular deflection is proportional to the displacement of its line of approach from the center of the slit. This means that the field is a cylindrical electron lens. If gradients exist on both sides of the slit, the focal length $f=(G_2-G_1)/2V_1$, V_1 being the voltage of the plate with respect to the thermionic source of the electrons. A hole in a charged plate was found to have a focal length of $(G_2-G_1)/4V_1$. We also devised means for experimentally determining the lens properties of apertures in charged plates. Essentially this consisted of photographing the trajectories in a tube containing a pressure of mercury vapor so low that ionic space charge effects were negligible. Figure 9 shows a series of such photographs for cylindrical lenses in concentric cylinders. The angular width of the slit in the first slide is 6 degrees, and the beam focuses at a voltage ratio of about 7.6. When the angular width is 12 degrees, focusing occurs at about 8.9 and at 18 degrees, at about 10.3. Similar tests were made on tubes with plates containing circular apertures (Fig. 10). As a result of these tests, we found the theoretical electron optical laws fulfilled provided the angular aperture was small, i.e., the F number was not less than 5. For small F numbers, aberration was in evidence, as seen in Fig. 9. The results of these investigations

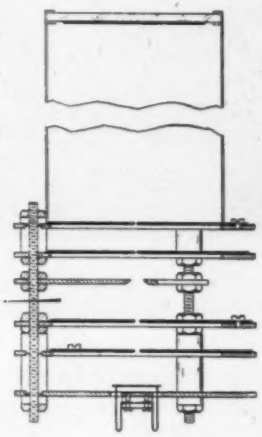

FIG. 11. Electron microscope.

were presented to the American Physical Society in 1931 and 1932.[14]

We then constructed an electron microscope (Fig. 11) in which two pairs of crossed wires were illuminated by electrons from the cathode below, through a lens system, a second lens system, and finally a fluorescent screen. Electron micrographs of cathode or of the crossed wires could be taken. From the latter, the magnification could be calculated, and Fig. 12 shows the close agreement obtained between theory and experiment when the angular aperture is kept small.[15]

Figure 13 shows an electron optical system devised by Davisson and Ahearn for the study of secondary emission at low primary electron energy. Electrons from the cathode are concentrated by a condenser lens system upon a thin foil containing a very small aperture, about 0.001″ diameter. A second lens system is used to collimate the electrons streaming through this aperture into a parallel beam which is incident upon the target. With this system, it is possible to explore the secondary emissive properties of surfaces down to primary energies of the order of magnitude of the thermal energy of the emitted electrons, since lateral components of electron velocity are negligible until the region of thermal energy is approached. This is an example of the electron-optical solution of the problem of producing an electron beam of known resolution, the problem which led to our electron-optical investigations.

FIG. 12. Electron micrographs of crossed wires showing agreement between theory and experiment.

In conclusion I would like to observe that electron optics, like its cousin geometrical light optics, is essentially a *tool* of science. Plebeian in its birth, it has maintained its character throughout its life as an engineering development rather than as a purely scientific advance. But the tools that applied science gives us make possible further advances into the unknown. And so electron optics is a tool enabling us to search more deeply into the great mysteries that are the province of pure science.

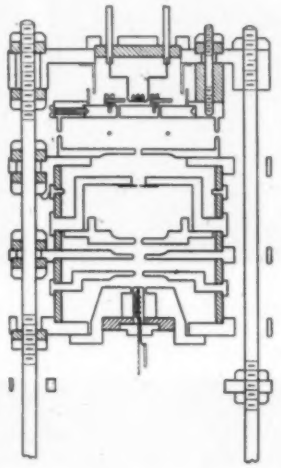

FIG. 13. Electron-optical system for study of secondary emission.

BIBLIOGRAPHY

(1) L. H. Germer and C. J. Davisson, Nature **119**, 558 (1927); Phys. Rev. **29**, 908 (1927).
(2) C. J. Davisson and L. H. Germer, Proc. Nat. Acad. Sci. **14**, 629 (1928); Phys. Rev. **31**, 708 (1928).
(3) L. H. Germer and C. J. Davisson, Phys. Rev. **33**, 118 (1929).
(4) J. J. Thomson, Phil. Mag. **44**, 293 (1897).
(5) Ferdinand Braun, Wied. Ann. **60**, 552 (1897).
(6) H. Busch, Ann. d. Physik **81**, 974 (1926); Archiv. f. Elektrotechnik **18**, 585 (1927).
(7) J. B. Johnson, J. Opt. Soc. Am. **6**, 701 (1922).
(8) M. Knoll and E. Ruska, Ann. d. Physik **12**, 607, 641 (1932).
(9) E. Brüche and H. Johannson, Naturwiss. **20**, 353 (1932).
(10) O. Scherzer, Zeits. f. Physik **80**, 193 (1933). See also J. Picht, Zeits. f. Instrumentenk. **53**, 274 (1933).
(11) H. Johannson, Ann. d. Physik **18**, 385 (1933).
(12) E. E. Watson, Phil. Mag. **7**, 849 (1927).
(13) V. K. Zworykin, J. Inst. Elec. Eng. **73**, 437 (1933).
(14) C. J. Davisson and C. J. Calbick, Phys. Rev. **38**, 585 (1931); **42**, 580 (1932).
(15) C. J. Calbick and C. J. Davisson, Phys. Rev. **45**, 764 (1934).

The Electron Microscope in Metallurgical Research*

CHARLES S. BARRETT

Metals Research Laboratory, Carnegie Institute of Technology, Pittsburgh, Pennsylvania

(Received June 26, 1944)

IN reviewing the applications of the electron microscope to metallurgical research, it would be proper to mention first the studies of the size and shape of colloidal powders. Many results in this field are of great commercial value and scientific interest, but since the techniques used and the nature of the photographs obtained have become familiar to physicists through frequent publication and through manufacturers' literature, they need not be treated here. This review is limited to metallographic studies with the electron microscope, in which the surface details of a polished and etched metal specimen are transferred to a replica and made visible in a transmission electron microscope, a procedure necessitated by the fact that the metallographic specimens are far too thick to be penetrated by electrons. The electron micrographs reproduced here to illustrate applications to physical metallurgy are selected from those made in the Metals Research Laboratory at Carnegie Institute of Technology in the past two years, using a type B2 RCA instrument.

SPECIMEN PREPARATION

Some excellent results have been obtained by the silver-collodion method of preparing replicas,[1,2] particularly on steel samples, but it has not come into general use because of the inconvenience of having to build up, by evaporation in a vacuum, a layer of silver thick enough to be stripped from the sample. (If a thin layer is evaporated and subsequently stiffened by electrolytic deposition, difficulties may be encountered, arising from the interaction of the electrolyte and the prepared surface.) After stripping, a collodion film is spread over the silver replica and by immersion in weak nitric acid the silver is etched away without attacking the collodion, which then becomes a replica suitable for electron microscopy.

A much more convenient method was developed by Schaefer and Harker[3] at the General Electric Company. A thin film of Formvar (polyvinal formal) dissolved in dioxane is spread over a freshly etched surface and stripped from the surface after drying. Figure 1a illustrates the results obtained by this Formvar method on pearlite in which the lamellae of ferrite and cementite are extremely thin. Disadvantages of the method are the difficulty of stripping from

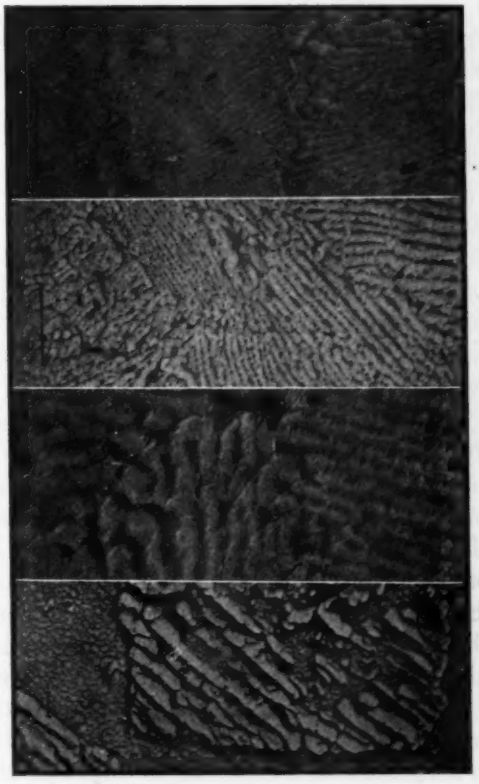

FIG. 1. Pearlite in rapidly cooled plain carbon steel. Line indicates 1μ, 10,000Å. (a) Formvar replica. Eutectoid steel. ×10,000. (b) Polystyrene-silica replica. Eutectoid steel. ×10,000. (c) Polystyrene-silica replica. Eutectoid steel. ×10,000. (d) Polystyrene-silica replica. Hypoeutectoid steel ×3,300.

* Paper presented at the inaugural meeting of the Division of Electron and Ion Optics of the American Physical Society at Pittsburgh on April 29, 1944.

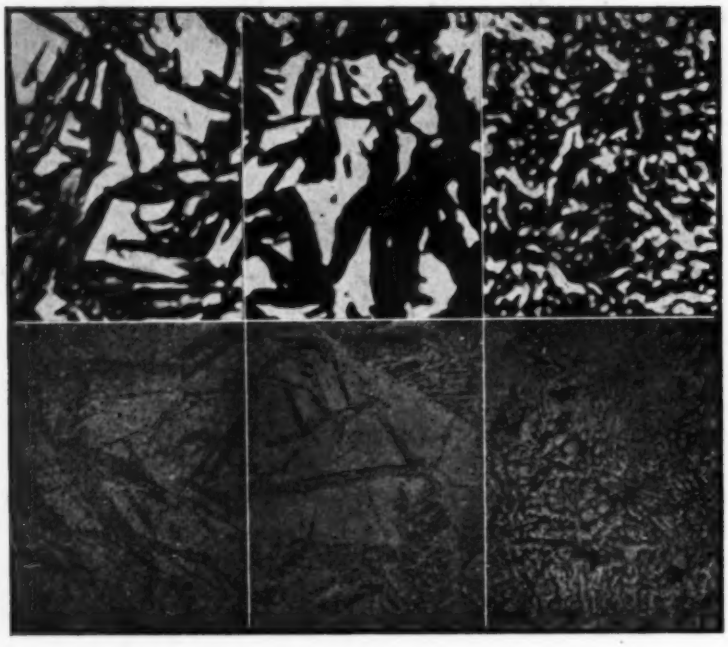

FIG. 2. Martensite in nickel steel (1 percent C, 4.82 percent Ni, 0.43 percent Mn, 0.05 percent S, 0.01 percent Si) nital etch. Top row, optical micrographs ×2000; lower row, electron micrographs ×2000. (a) Tempered 5 min. at 175°C; 52 Rc hardness; 50 percent austenite. (b) Tempered 5 min. at 290°C; 52 Rc; 25 percent austenite. (c) Tempered 5 min. at 370°C; 48 Rc; 0 percent austenite.

rough and deeply etched surfaces and the extreme cleanliness required of the prepared surface to permit satisfactory wetting of all areas. The resolution obtained is good, but somewhat less than can be had with the method next to be discussed.

Heidenreich and Peck at The Dow Chemical Company developed a double-replica method that seems the most satisfactory to date.[4] A thermoplastic material, polystyrene, is molded into the prepared surface by applying a pressure of 3000 pounds per square inch and a temperature of 150°C. After cooling, the plastic molding is separated from the metal, usually by cleavage, and mounted in an evacuated bell jar where a thin layer of silica is deposited upon it by evaporating a piece of quartz in a small electric furnace. When a layer a few hundred angstroms thick has been deposited, the molding is placed in a liquid (ethyl bromide later diluted with benzene) that dissolves the plastic and leaves the thin silica film swimming in the solvent. The almost invisible film is then caught on a fine wire mesh and transferred to the microscope, where its variations in thickness provide a replica of the details on the surface of the metal specimen.

Except where noted otherwise, all of the accompanying micrographs were made with this method. It, too, presents difficulties of various kinds. The most common artifacts encountered with this method have been illustrated in another paper.[5] Staining of the specimen during the

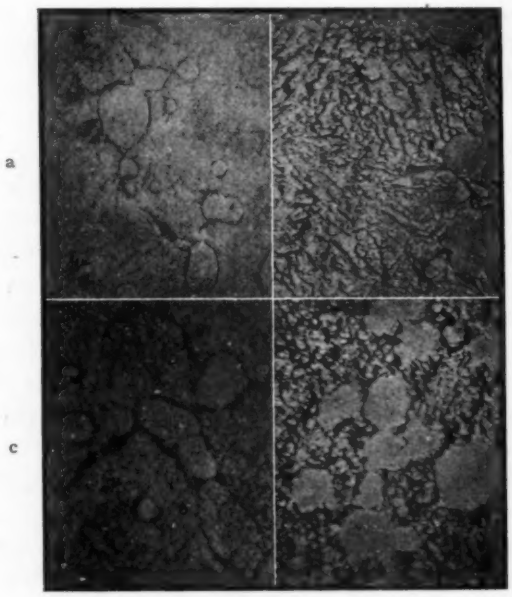

FIG. 3. High speed steel, electron micrographs, nital etch ×2500. (a) As quenched. Hardness Rc 65.6. (b) Undertempered (1 hr. at 265°C, 510°F) Rc 60.8. (c) Properly tempered (1 hr. at 550°C, 1020°F) Rc 64.5. (d) Overtempered (1 hr. at 700°C, 1290°F) Rc 46.2.

polystyrene molding is not uncommon, but can be minimized if all traces of the etchant are removed by thorough washing before molding, and if reasonably fresh polystyrene is used. Folds and tears are easily recognized; "rings" are associated with moisture condensation and may be avoided, as Heidenreich has shown, by the addition of benzene to the bath before fishing out the silica replica; imperfect cleavages that produce "styrene lines" can readily be recognized. It is probable that all replicas undergo a progressive alteration while in the microscope because of the deposition of organic material from the electron beam. This is familiar to those who have used the microscope on small particles, but is not usually considered by the metallographer. The loss of detail and resolution from this cause should be minimized if the time the specimen is in the electron beam is kept small, and if the beam intensity is kept down.

The use of oxide films for replicas,[6] reviewed in another paper of this symposium, has proved useful for certain alloys, particularly aluminum alloys, where suitable natural or artificial films can be produced.

EXAMPLES OF RESULTS

Pearlite

The structure of pearlite in steel, so familiar to metallographers, is always a good subject to begin on, for its fineness can be varied over wide ranges without essentially altering its appearance. Figures 1a and 1b, showing pearlite lamellae of minimum spacing, closely resemble optical micrographs, and Fig. 1c shows an echelon arrangement of jagged edged lamellae of cementite (Fe_3C) which doubtless appear in relief because the etchant (0.5 percent nital) has etched away the intervening ferrite. Figure 1d shows again the unetched plates of cementite projecting from the background of etched ferrite, in a steel of lower carbon content (0.76 percent C). Interlamellar spacings from pictures of this kind[5] are in agreement with values obtained by less direct means.[7] The unresolved structure that used to be frequently referred to as nodular troostite is easily resolved in electron microscopes into lamellar and cellular structures, as in Fig. 1, which are clearly pearlite.

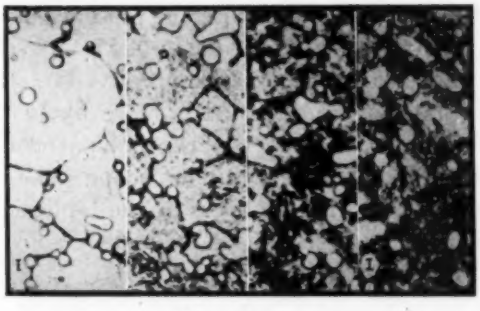

a b c d

FIG. 4. Optical micrographs of the same samples as Fig. 3(a, b, c, d), respectively, ×1250.

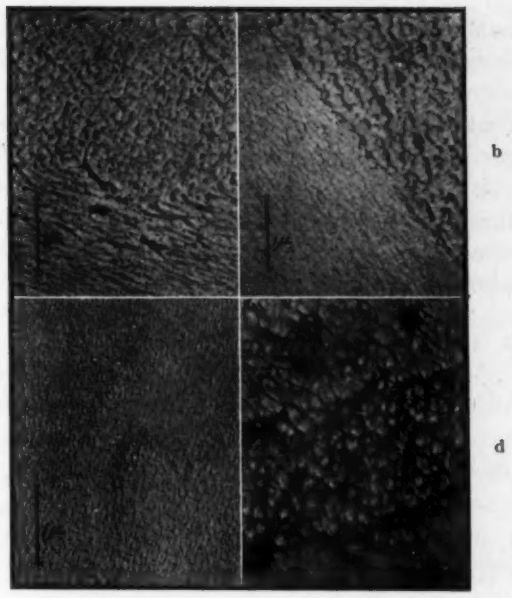

FIG. 5. Age hardening *K* monel metal with various heat treatments. Electrolytic etch ×10,000. (a) As quenched in water, 161 Brinell hardness. (b) As quenched in iced brine. (c) Aged to maximum hardness, 301 Brinell hardness. (d) Overaged, 255 Brinell hardness.

Martensite

Tempered martensite in steels has proved to be a most difficult subject to study, because of the uncertainty as to what its appearance at high magnification should be and because of the many different appearances found on electron micrographs. A direct comparison of optical and electron micrographs at the same magnification, as in Fig. 2, is perhaps the best guide in distinguishing true structures from false. The darkened martensite "needles" of the optical micrographs are resolved in the electron micrographs into roughened lenticular areas surrounded by smooth

austenitic areas. The scale of the roughness progresses from fine to coarse as the tempering is increased, perhaps indicating a growth and coalescence of carbide particles. However, no precipitated carbide particles can be distinguished in the pictures, and in none of these three samples were x-ray diffraction lines from cementite found, according to Dr. M. U. Cohen, who furnished them.

High Speed Steel

A successful series of pictures was obtained of high speed steel (Fig. 3)—defining successful as meaning understandable in terms of the ordinary photomicrographs of Fig. 4. Unetched carbide crystals are white and smooth, easily recognized; a properly tempered sample shows what are believed to be finely divided precipitated particles between the large carbides (Fig. 3c) where undertempered and overtempered samples show merely a general roughening from the etchant, as in other martensites, such as would cause the martensite to appear dark under the microscope.

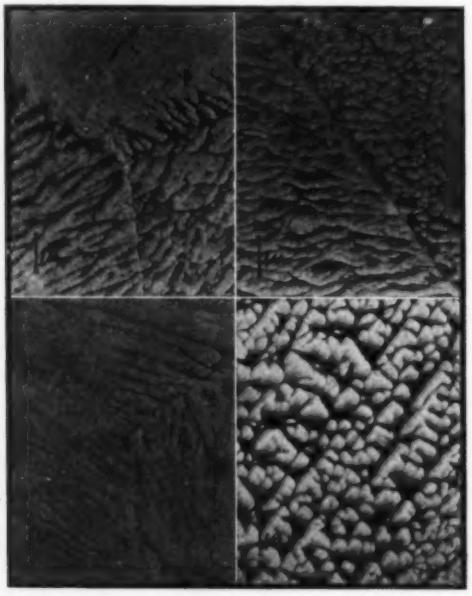

FIG. 6. Etched high purity copper, annealed, ×5000. a, b, c, etched with potassium dichromate-sodium chloride-sulfuric acid etchant, d, with ferric chloride-hydrochloric acid. Grain boundaries shown in a, b, and c.

Age Hardening Alloys

Unquestionably the electron microscope can often contribute to our knowledge of the microstructure of age hardening alloys, for in many alloys the maximum hardening effect occurs at a stage when the precipitated crystals responsible for the hardening are of submicroscopic dimensions. The series of prints in Fig. 5 shows details developed in the aging of *K* monel (66 percent Ni, 29 percent Cu, 1 percent Fe, 2.75 percent Al), which are invisible in photomicrographs. At maximum hardness, Fig. 5c, there are many small particles spaced no more than 300 angstroms apart. These have apparently coalesced, in Fig. 5d, into larger particles. The band across the picture in Fig. 5d is a twin, 1.6 μ wide, which, because of its different orientation, has altered the attack of the etchant; boundaries between grains are also seen in Figs. 5a and 5b.

Copper

The etched surface of a single-phase metal or alloy frequently exhibits a structure of remarkable interest as will be seen from Fig. 6 of etched polycrystalline copper. It seems probable that the effects are due to variation in perfection of the crystalline grain, since the patterns obviously change with the grain orientation.

The attack of the etchants appears to be most rapid along the boundaries of rod-shaped domains that are 0.1 to 0.5 μ in diameter (1000 to 5000 angstroms) and up to 5 μ long. In monel metal there appear to be similar domains, smaller, forming equiaxed blocks 0.05 to 0.1 μ in diameter. One is tempted to associate the hardness of a single-phase metal with the fineness of this etching structure, and also to associate these domains with those that have been discussed in theories of dislocations, x-ray diffracting power, and studies of x-ray line widths, but the significance of the correlation has yet to be proved.

It must be admitted that the presence of these relatively coarse etch patterns is a serious hindrance to electron metallography. The resolution that can be obtained is more likely to be limited by the coarseness of the etch pattern than by the resolution of the microscope (30 to 100 angstroms) or the thickness of the replicas (300 to 600 angstroms). This is eloquently shown by the pictures of brass.

Brass

Cartridge brass, after being deformed, polished, and etched, yields photomicrographs in which

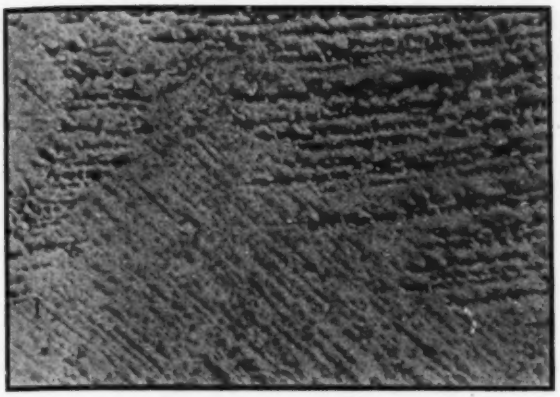

FIG. 7. Cold-worked cartridge brass, polished and etched. ×2500.

most of the grains are crossed by fine lines, the nature of which has long been under discussion by metallurgists. Judging from Fig. 7 the widths of individual lines and their behavior at cross-over points cannot be learned until a method of etching is developed that produces much finer etch pits. A standard metallographic etchant was used here, and the electron micrographs can scarcely be said to yield more information than ordinary photomicrographs.

SLIP LINES

The electron microscope offers an excellent opportunity to study the surface contour of crystals after deformation. In Fig. 8 are electron micrographs of metal surfaces that were first given a metallographic polish, etched, then deformed slightly, and finally reproduced by the polystyrene silica replica method. Slip lines that intersect the surface nearly perpendicularly produce a stepped surface with sharp edges, as if the deformation at each step is confined to a plane or to a zone less than 200 or 300 angstroms wide. (Just how much less than this is difficult to determine.) There is no evidence of closely grouped slip lines at each major step. The single grain of brass shown in Fig. 8a may contain some deformation twins as well as slip lines, for deformation twins could account for the lines that are not effaced by subsequent polishing and etching—the lines of Fig. 7. Both slip and twinning should delineate planes of the form (111), and identification of one from the other is uncertain. Figure 8b of monel metal shows broad bands of fresh metal that has been exposed by the displacement along slip planes. When a specimen is elongated by plastic deformation it is the underlying metal, brought to the surface in this way, that increases the external surface of the specimen. Against the side of such a band one can see the contours of intersecting slip lines, somewhat confused, of course, by the etching that had been given the piece prior to deformation. The displacement at the widest band is about 0.7 μ. In Fig. 8c slip lines are seen in two grains of copper.

CONCLUSION

Experience up to the present time suggests that new metallographic polishing and etching techniques are needed; for example, a few tests have indicated that the newer electrolytic polishing sometimes gives better results than mechanical polishing, while standard etching techniques often produce much too coarse etch pits. Much has been accomplished in developing methods of making replicas, but the yield of successful replicas is small, even with the most routine samples, and the labor involved far exceeds that required for optical metallography. Optical examination must almost invariably precede elec-

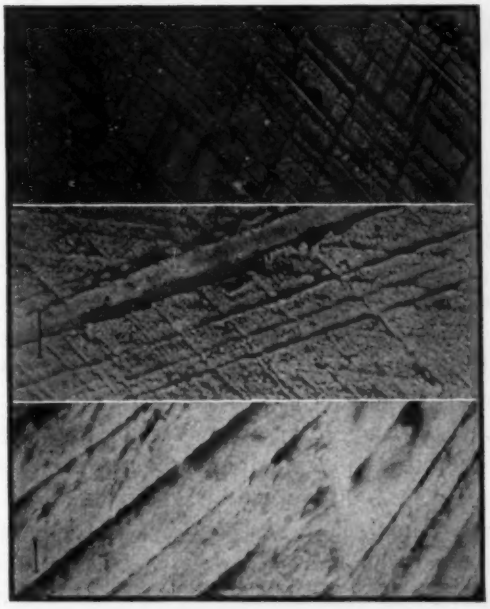

FIG. 8. Slip lines on polished and etched metals. (a) Cartridge brass ×2000. (b) *K*-Monel metal ×6000. (c) High purity copper ×4000.

tron work as an aid to interpretation and as a control of the metallographic procedure, which must be carried out with the care and skill of high power optical metallography. The resolution that can be attained is remarkable even with replicas, and high magnification is therefore possible. It is best, however, to take electron micrographs at a low magnification and subsequently enlarge when printing, and a final magnification of 2500, 5000, or 10,000 is generally preferable to higher magnifications that give very small fields of view.

REFERENCES

(1) V. K. Zworykin and E. G. Ramberg, J. App. Phys. **12**, 692 (1941).
(2) R. F. Mehl, Trans. Am. Soc. Metals **29**, 813–862 (1941).
(3) V. J. Schaefer and D. Harker, J. App. Phys. **13**, 427–433 (1942); V. J. Schaefer, Phys. Rev. **62**, 495–496 (1942).
(4) R. D. Heidenreich and V. G. Peck, Phys. Rev. **62**, 495–496 (1942); J. App. Phys. **14**, 23–29 (1943). R. D. Heidenreich, J. App. Phys. **14**, 312–320 (1943).
(5) C. S. Barrett, Tech. Pub. 1637, Metals Tech. **10** (Sept. 1943).
(6) A. Mahl, Zeits. f. tech. Physik **21**, 17–18 (1940); F. Keller and A. H. Geisler, Tech. Pub. 1700, Metals Tech. **11** (April, 1944).
(7) R. F. Mehl, Trans. Am. Soc. Metals **29**, 813–862 (1941).

Extending Microscopic Examination of Metals*

BY F. KELLER AND A. H. GEISLER

Metallography Division, Aluminum Research Laboratories, Aluminum Company of America, New Kensington, Pennsylvania

(Received May 17, 1944)

MICROSCOPIC examination has provided much useful information about the structure and behavior of metals and alloys. Some important changes in structure, however, have been unresolvable by the light microscope and could not be studied metallographically. This is especially true of the changes in structure associated with age hardening of some aluminum alloys. In this case, precipitate particles ranging in size from 1000A down to about 10A are of interest. Thus, there has been a real need for a microscope which would resolve very fine structures for work in this range.

Metallurgists now have available a new and important tool in the electron microscope. This instrument with a resolving power of less than 25A furnishes a new and useful means for the evaluation of the fine structure of metals in a range not possible heretofore and for greatly extending the field and usefulness of microscopic examination.

* Paper presented at the inaugural meeting of the Division of Electron and Ion Optics of the American Physical Society at Pittsburgh on April 29, 1944.

ELECTRON MICROSCOPES

Several different types of electron microscopes[1] have been applied to study the structure of metals and alloys. These are: (1) the emission type in which the sample serves as the cathode to furnish electron emission, (2) the reflection type wherein the radiation reflected by the surface of the sample is used to form an image which is magnified by electronic lenses, (3) the scanning microscope in which the surface of the sample is scanned by a very small beam of electrons and the secondary radiation emitted by the sample actuates a facsimile printer in synchronism with the movement of the electronic probe, and finally (4) the transmission type of electron microscope in which the path of the electrons is analogous to that of the light path in the transmission light microscope. This microscope has high resolving power and probably gives the best results with the techniques that are now available.

LIMITATIONS OF TRANSMISSION MICROSCOPE

Results with the transmission type of electron microscope are controlled largely by limitations

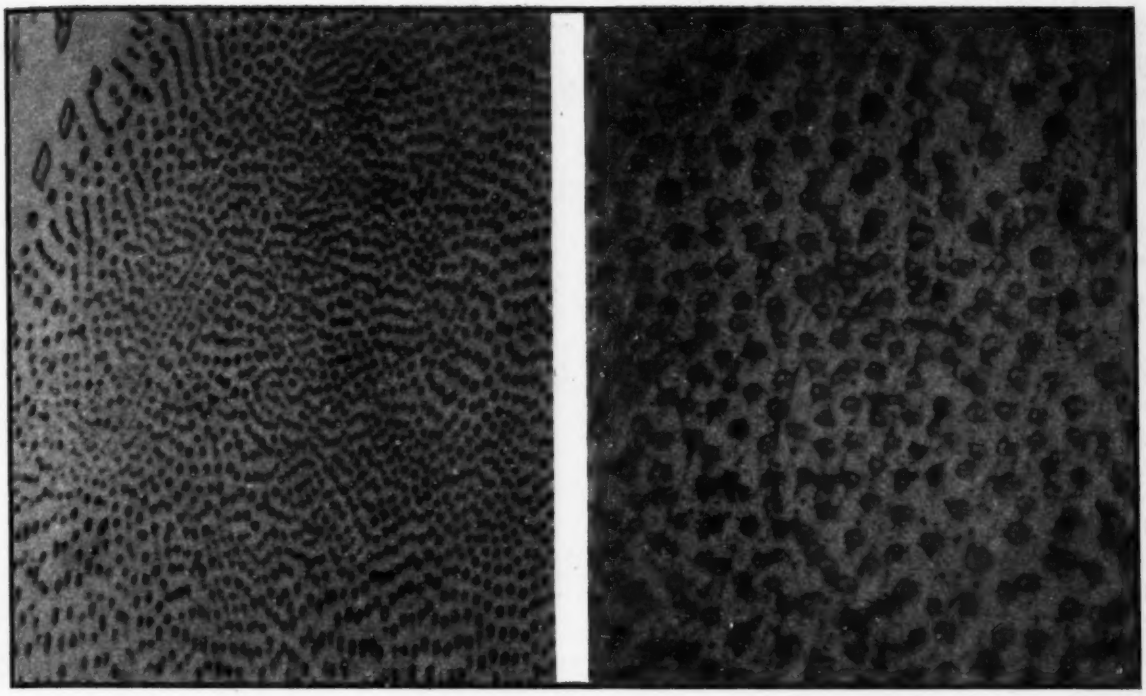

FIG. 1. Light micrograph showing eutectic structure of a polished and etched specimen of a chill cast aluminum alloy containing 3.5 percent iron. The $FeAl_3$ particles are barely resolvable in some regions. Mag. 1500×.

FIG. 2. Electron micrograph of a silica replica from the same sample. The shape and spacing of the particles are well defined. Mag. 4000×.

of particle size, shape discrimination, and degree of contrast. The first two limitations depend on the resolving power of the microscope, the last largely on the characteristics of the samples. A resolving power about 100 times better than that obtainable with the light microscope—20 to 40A—can be obtained with transmission microscopes equipped with electromagnetic lenses and values 10 times better—200 to 400A—are reported for those equipped with electrostatic lenses.

A structure in which the particle sizes and spacings are near the limit of resolution with the light microscope is shown by Fig. 1. These fine particles appear as solid black dots of circular shape without definite outline. The shape, outline, and spacing of these particles, however, are readily apparent upon examination of a replica from the same sample with the electron microscope as shown by Fig. 2. Thus, the second limitation, shape discrimination, has been demonstrated in relation to resolving power.

With a given resolving power, the greater the number of straight sides a particle has in the plane of observation, the larger the particle must be in order that its shape can be distinguished from a circle. Calculations with an equation suggested by Borries and Kausche[2] indicate that with a resolving power of 25A, square particles should have an area of at least 7280 sq. A (85A on the side); whereas, octagon-shaped particles should have an area of at least 44,600 sq. A (96A on the side) or the particles will appear as circles. Images of particles of the above sizes will appear to have rounded corners but the geometrical shape of the particles can be recognized.

The third limitation involves differences in contrast between the images of the material under examination and the background. A difference of about 10 percent or greater in contrast is required or the image will not register satisfactorily on the photographic plate. Thus, thin flat particles lying perpendicular to the electron beam may not be detectable regardless of their lateral dimensions if they scatter less than about 10 percent of the incident radiation.

Image contrast which depends on the relative thickness of the material, on its density, on the scattering power of its component atoms, and on

the speed of the electrons used is probably as important a factor in the results obtained with the electron microscope as the resolving power. The significance of this limitation is mentioned in the section wherein the various methods available for specimen preparation are described.

APPLICATION OF ELECTRON MICROSCOPE IN METALLURGY

Metallurgists are interested in the grain structure and intermetallic phases in alloys and the effects of various mechanical and thermal treatments on these features. Unfortunately, the transmission type electron microscope is not adaptable for the examination of metallic samples directly because the specimens would have to be reduced to a thickness that is impractical. To circumvent this difficulty, however, a number of unique methods have been devised for producing a thin specimen that represents faithfully the structure of the prepared surface of a metal specimen.

FIG. 3. Electron micrograph of Formvar replica from an electropolished specimen of a heat treated aluminum alloy containing 4.5 percent copper which was aged ½ hr. at 250°C. Mag. 20,000×.

The methods available for preparing specimens of metallic samples for use with the transmission type of electron microscope fall into two main categories: (1) the replica methods in which either a negative or positive reproduction of the surface of the sample is obtained on a very thin film, and (2) the oxide film methods in which the actual metal surface is converted into a thin oxide film by some thermal, chemical, or electrochemical treatment and subsequently stripped from the metal sample. Both methods, in general, owe their origin to Mahl;[3] however, new and improved techniques for preparing samples are being presented continually.

FIG. 4. Electron micrograph of Formvar replica from electropolished specimen of heat treated aluminum alloy containing 4.5 percent copper which was aged 24 hr. at 250°C. Mag. 20,000×.

REPLICA METHODS

With the replica method, one surface of the thin replica follows the original contour of the etched surface of the sample while the other surface remains flat. Replicas are made by forming a thin film of some inert material on the prepared surface of the sample. This film is formed directly on the surface in the case of a negative replica and on a reproduction of the original surface in the case of a positive replica. Variations in the contour of the surface of the sample, therefore, caused mainly by etching produce variations in the thickness of the replica. These are responsible for contrast and tones in the image obtained. Thus with replicas, the contrast limi-

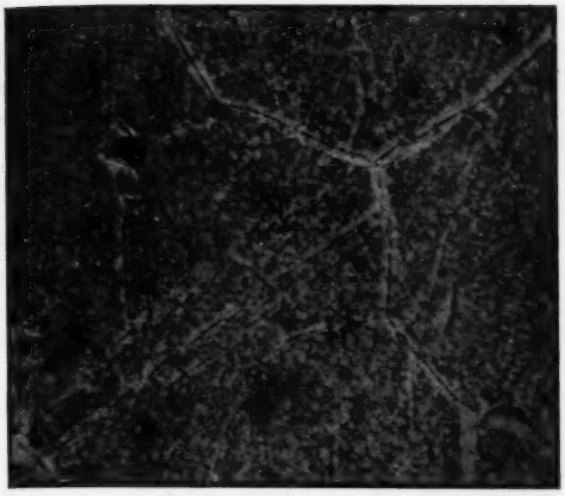

FIG. 5. Electron micrograph of silica replica from polished and etched specimen of magnesium-base alloy AM-C52S-H. The grain and twin boundaries are well reproduced by the silica replica. Mag. 4000×.

tation is introduced when the differences in thickness are insufficient to give good contrast.

The negative type of replica is readily made by flowing solutions of lacquers such as collodion[3] or Formvar[4] on to the polished and etched surface of a sample. The thickness of the film obtained is a function of the concentration of the solution. Thin metallic films formed by evaporation of aluminum and beryllium and other metals have been used as replicas but some of these films tend to have an undesirable granular structure which may obscure the structure of the sample under examination.

Regardless of the material used, the thin replica film is removed from the sample either by mechanical or chemical methods and is examined in the electron microscope to obtain the fine structure of the surface of the original metallic sample. Examples of electron micrographs of negative replicas from an aluminum-copper alloy are shown in Figs. 3 and 4. The structure shows $CuAl_2$ particles that have been precipitated in a regular pattern from the solid solution matrix by an aging treatment at an elevated temperature. Cross sections of the $CuAl_2$ plates appear as white streaks corresponding to thin areas in the replicas. The contrast which depends on thickness differences alone as shown in Fig. 3 is rather poor; it is much better in Fig. 4 because many of the plates have dark particles along them which are probably etching products that adhered to the replica. Here the contrast is better because the difference in density between the particles and the background is sufficient to give good definition.

The positive replica method involves the use of a more complex two-stage process but it yields a replica with high and low points that correspond directly to those of the original metallic sample. First a negative impression is obtained of the surface, then a thin positive replica is made from the initial mold. The original positive replica method[5] consisted in electrodepositing a layer of silver on the polished and etched surface of a sample. The silver coating is removed mechanically and a collodion solution is flowed onto the replica surface of the silver. The thin collodion film is then removed by dissolving the silver with nitric acid.

A more recent positive replica method[6] consists in using polystyrene for the first impression and an evaporated silica film for the replica. With this method, an impression of the prepared surface is made in polystyrene. The metal specimen is then removed from the impression by mechanical stripping or chemical solution. Then a

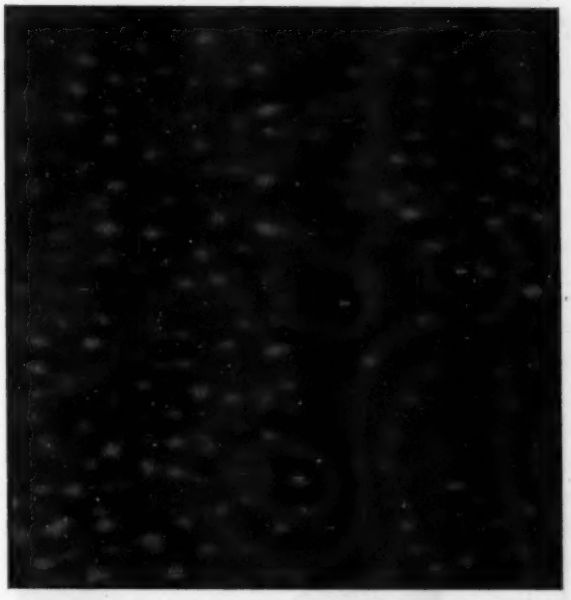

FIG. 6. Electron micrograph showing structure of the oxide film formed on 99.95 percent aluminum by an anodic oxidation treatment in a phosphoric acid electrolyte. Mag. 110,000×.

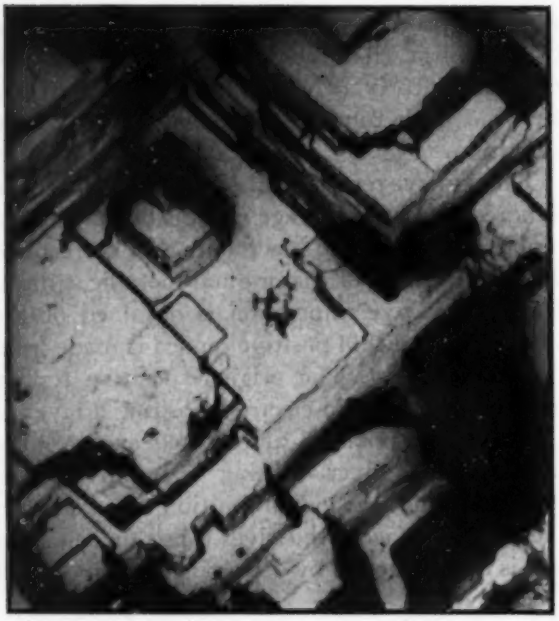

FIG. 7. Electron micrograph of oxide film from a deep-etched annealed aluminum sheet specimen showing well-developed cubic block structure within a single grain. Mag. 8000×.

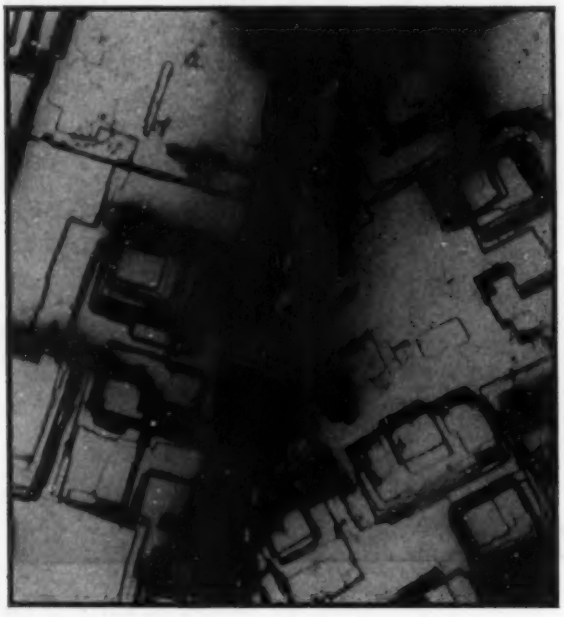

FIG. 8. Electron micrograph of oxide film from a deep-etched annealed aluminum sheet specimen showing cubic block structure adjacent to a grain boundary. Mag. 8000×.

very thin layer of pure silica is evaporated onto the surface of the polystyrene impression. The thin silica film which gives a positive replica of the original metal surface is subsequently removed by dissolving the polystyrene with ethyl bromide. The results obtained with silica replicas of the type just described are illustrated by the electron micrographs, Figs. 2 and 5.

The particles of $FeAl_3$ in an aluminum-iron alloy shown by Fig. 2 are represented by somewhat grayer areas than the matrix. This is the result of the particles being slightly in relief after polishing and etching. The best differentiation, however, is afforded by the dark outline around the particles which resulted from selective etching of the matrix adjacent to the particles. In Fig. 5, the results obtained from a silica replica of the surface of a magnesium alloy are shown. The grain and twin boundaries are well reproduced by the silica replica. The general mottling within the grains, however, was probably caused by a discontinuous etching film that remained on the polystyrene mold. This represents an undesirable residue of etching products; whereas, those in Fig. 2 helped in producing contrast. Other examples of the use of these replica methods for examination of metallographic samples may be found elsewhere.[7]

FIG. 9. Light micrograph of a deep-etched annealed aluminum sheet specimen. With the light microscope, it is not possible to show very much detail of the block structure because of inability to obtain sufficient depth of focus. Mag. 500×.

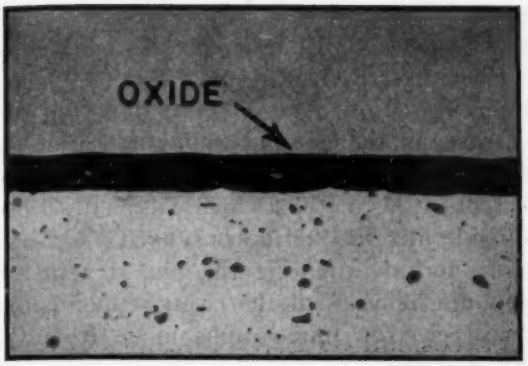

FIG. 10. Light micrograph of a cross section of an anodically coated aluminum alloy containing 5 percent silicon. Since the silicon particles are not affected by the oxidation treatment, they remain in place in the oxide coating. Mag. 500×.

OXIDE FILM METHOD

Whereas the replica methods are applicable to any metal or alloy, the oxide film method is limited at present to use for those metals for which satisfactory film formation and removal techniques are known. The methods will vary with different metals and no single method is universally applicable.

For aluminum alloys, oxide films formed by electrochemical action have been found the most suitable for electron microscope specimens. Those formed by heating or chemical action are not suitable because of their porous structures. To make suitable oxide films on aluminum alloys, the sample is made anode in a suitable electrolyte and a potential is applied. The thickness of the oxide film obtained is influenced by the applied voltage, the time of treatment, and by the concentration, temperature, and type of electrolyte. In electrolytes such as solutions of borax-boric acid, sulphuric acid, oxalic acid, or phosphoric acid, a pore structure characteristic of the oxide[8] is usually developed which interferes with the microstructure of the metal surface as shown by Fig. 6. Two anodic oxidation treatments employing borax-boric acid and ammonium borate have been used successfully by early investigators, but under some conditions undesirable oxide structures are obtained with these electrolytes.

To form more suitable oxide films on aluminum alloys for use as electron microscope specimens, a new technique was developed by the authors.[9] The oxide films are made by an anodic oxidation treatment in an electrolyte containing 12 percent disodium phosphate (Na_2HPO_4) and 0.4 percent sulphuric acid in water. Potentials of 20 to 40 volts are used and oxide films of satisfactory thickness (500–700A) for electron microscope specimens are obtained with a 3 to 5 minute treatment. No characteristic oxide structure has been detected in these films at magnifications up to 100,000 times.

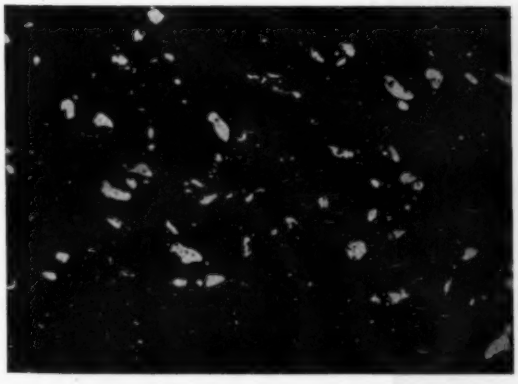

FIG. 11. Light micrograph of the oxide film after it had been removed from the sample. This was made with vertical reflected light and shows the silicon particles embedded in the oxide. Mag. 500×.

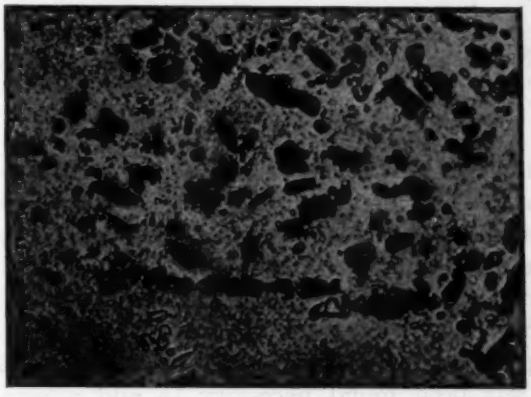

FIG. 12. Light micrograph of same sample shown in Fig. 11 made with transmitted light. Mag. 500×.

Removal of these oxide films from the aluminum specimens is accomplished readily by using the mercury method. A network of lines about $\frac{1}{8}$" apart is scribed on the oxidized surface to cut the film into small squares. The sample is immersed in a saturated solution of mercuric chloride for about 30 seconds to allow mercury to deposit on the exposed aluminum along the scratches. The

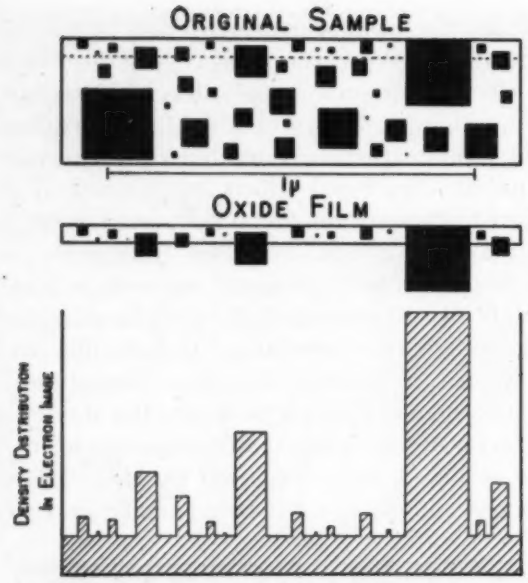

FIG. 13. Schematic diagram showing effect of constituent particles in oxide film on density distribution in electron microscope image.

sample is then removed and placed in distilled water. The deposited mercury dissolves the aluminum at the interface and thus undermines the oxide film. The small squares of oxide film soon float free from the aluminum and can be removed from the water bath with the specimen supporting screens. With certain aluminum alloys, it has been found necessary to add a small amount of the mercuric chloride solution to the distilled water. Satisfactory pieces of oxide film have been removed from many different aluminum alloys.

Because of the ease of forming and removing aluminum oxide films and of certain advantages inherent in this method which will be described, the oxide film method is considered very satisfactory for investigating the fine structure of aluminum alloys with the electron microscope. Typical electron micrographs made from this type of oxide film specimen are illustrated by Figs. 7, 8, and 14–16.

CHARACTERISTICS OF OXIDE FILMS

Use of oxide films instead of replicas for aluminum alloys is advantageous because of the manner in which two important microstructural features—surface contour and constituent particles—are portrayed in the electron micrographs. These oxide films, like the various replicas, will faithfully reproduce the contour of the surface of the metal specimen. This is apparent from Figs. 7 and 8 which show the block structure of aluminum that is developed by deep etching.[10] Comparison of Figs. 7 and 8 with Fig. 9 not only shows the similarity of structures as revealed for the actual sample by the light microscope and for the oxide film specimen from the same sample by the electron microscope but also demonstrates

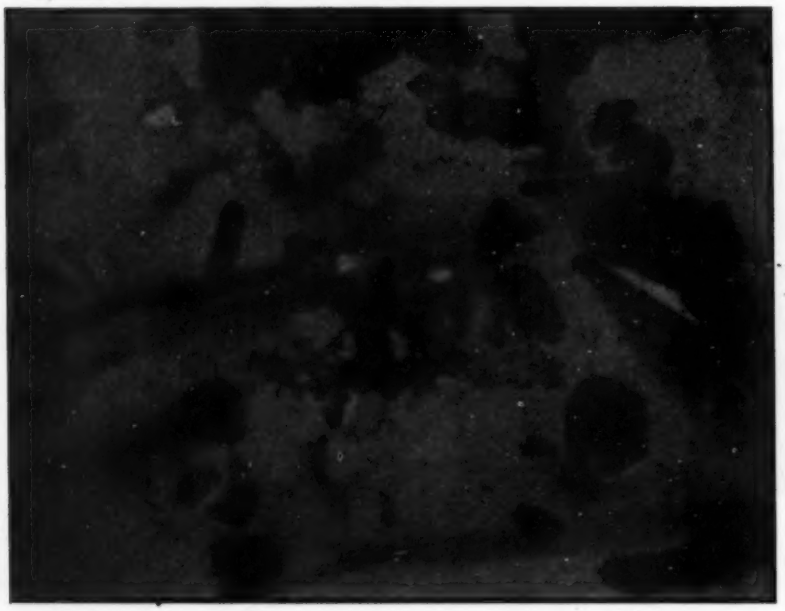

FIG. 14. Electron micrograph of oxide film from a deep-etched specimen of an aluminum alloy containing 1.23 percent silicon. The plate-shaped silicon particles are either occluded in or attached to the oxide film. Mag. 40,000×.

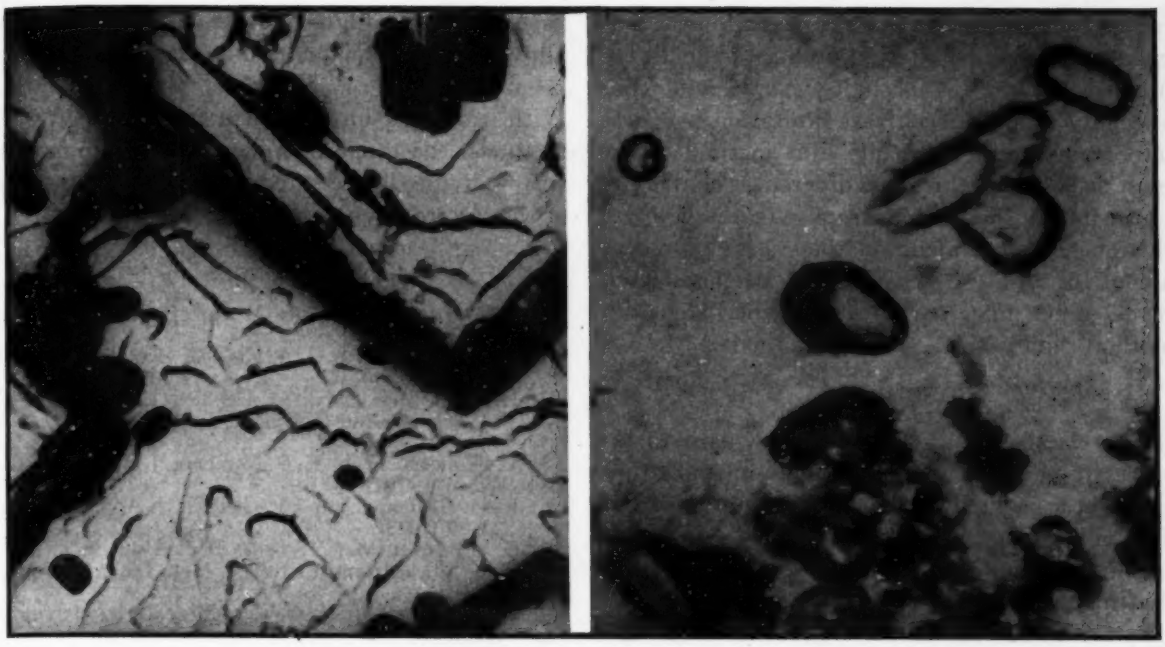

FIG. 15. Electron micrograph of oxide film from an annealed commercial aluminum alloy containing 1.25 percent manganese showing structure developed by deep-etching and constituent particles. Mag. 16,000×.

FIG. 16. Electron micrograph of oxide film from a metallographically polished and etched sample of the same material shown in Fig. 15. The outlined cavities represent the same constituent that appears dark in Fig. 15. Mag. 16,000×.

the usefulness of the electron microscope for examining these structures. In addition to resolving details finer than those resolvable with the light microscope, the electron microscope, because of its relatively small numerical aperture and large depth of focus, is capable of showing at high magnification the different levels within the grains and at the grain boundaries of the deep etched samples.

Contrasts or differences in brightness in the electron image of the oxide film depicting surface contour alone originate from the incident angle that the various plane elements make with the electron beam. As the angle between the surface element of the oxide film and the electron beam decreases, the distance through the oxide film traversed by the electron beam increases and the intensity of the electron image decreases. Thus surface elements normal to the electron beam appear bright, those parallel appear black, whereas those at intermediate angles appear various shades of gray as shown by Fig. 7.

The greatest advantage of the oxide film method originates in the behavior of the microconstituents during the formation and removal of the oxide films. During the anodic oxidation of aluminum alloys, some of the microconstituents are not oxidized or attached as shown in Fig. 10; some are oxidized partially; others are readily oxidized or dissolved.[11] Thus, the oxide film may contain occluded or affixed particles of unchanged constituents as shown by Figs. 11 and 12, particles of oxidation products of constituents, or voids from which the constituents have been dissolved. In all cases, however, evidence of the various phases is apparent in the electron image regardless of whether or not the particles were etched below the general surface level of the sample.

The best results are obtained with the oxide film method when the constituent particles or their oxidation products are occluded in or affixed to the oxide film as shown schematically by Fig. 13 and in the electron micrographs in Figs. 14 and 15. The latter show images from particles of silicon and aluminum-manganese constituent, respectively. Under these conditions, the contrast in the electron microscope image is controlled not only by differences in the electron path through the oxide film from surface contour (as with the

replica methods or as in Fig. 16) but also by differences in electron scattering ability of the aluminum oxide and the occluded particles of constituent. Thus, the contrast limitation is of less importance with the oxide film method where both density and thickness differences contribute to the image than with the replica methods where the image is dependent on thickness differences alone. In this respect, it should be possible to reveal much finer particles with the oxide film method than with the replica methods.

CONCLUSIONS

The electron microscope is being used to investigate the structure of aluminum and other alloys in a range far below the resolution of the light microscope. The results have been rather encouraging and there is every reason to believe that much new and useful information on other alloys will be obtained when the unusually high resolving powers of the electron microscope are more fully utilized. Although the illustrations in this paper are limited to results on aluminum alloys, similar and equally important results have been obtained on other metals and alloys. With continued improvement in equipment and methods, the range of microscopic examination will undoubtedly be extended greatly by the use of the electron type of microscope.

REFERENCES

(1) C. Marton and S. Sass, J. App. Phys. **14**, 522–531 (1943).
(2) B. von Borries and G. A. Kausche, Kolloid Zeits. **90**, 132–141 (1940).
(3) H. Mahl, Metallwirts. **19**, 488–491 (1940).
(4) V. J. Schaefer and D. Harker, J. App. Phys. **13**, 427–433 (1942).
(5) V. K. Zworykin and E. G. Ramberg, J. App. Phys. **12**, 692–695 (1941).
(6) R. D. Heidenreich and V. G. Peck, J. App. Phys. **14**, 23–29 (1943).
(7) C. S. Barrett, Met. Tech. **10** (Sept. 1943).
(8) J. D. Edwards and F. Keller, Met. Tech. **11** (April, 1944).
(9) F. Keller and A. H. Geisler, Met. Tech. **11** (April, 1944).
(10) H. Mahl and I. N. Stranski, Naturwiss. **31**, 12–17 (1943).
(11) F. Keller, Proc. A. S. T. M. **40**, 948–958 (1940).

The Magnetically Focused Radial Beam Vacuum Tube*

BY A. M. SKELLETT

Bell Telephone Laboratories, Inc., Whippany, New Jersey

(Received June 27, 1944)

A new type of vacuum tube is described in which a flat radial beam of electrons in a cylindrical structure may be made to rotate about the axis. Features of the tube are the absence of an internal focusing structure and resultant simplicity of design, its small size, its low voltages, and its high beam currents. The focusing of the beams and their directional control are accomplished by a magnetic field.

THE many proposals that have been made in the past few years for the use of electron beams in functions of the switching variety have focused attention on the need for a new kind of vacuum tube. Most such proposals have been impractical because of the unsuitability of the cathode-ray type of tube for this kind of use. The type of tube described herein is designed primarily for use in applications of this sort; it operates on low voltages and produces high beam currents so that it is essentially a low impedance device and it has wide angular control and good efficiency.

The elementary tube structure is shown in Fig. 1. The cylindrical cathode, which is of the variety commonly used in vacuum tubes, is surrounded by a coaxial cylindrical anode structure. Two types of electric field are used. The first has cylindrical symmetry and is obtained by putting

* Paper presented at the inaugural meeting of the Division of Electron and Ion Optics of the American Physical Society at Pittsburgh on April 29, 1944.

the same potential on all of the anode elements making them positive with respect to the cathode. The second is a uniform electric field obtained by varying the potential of the anode elements according to the cosine of the angle taken around the axis. The cathode is at zero potential. This potential distribution gives the same sort of electrostatic field in the tube as would be obtained between two parallel plates with the cathode located halfway between them both electrically and physically.

For the first type, i.e., the cylindrical field, a uniform magnetic field applied with the lines of force parallel to a diameter focuses 85 to 90 percent of the electrons into two beams parallel to the lines of magnetic force as shown in Fig. 1. The other 10 to 15 percent of the space current is lost at the cathode because of the added space charge that is due to the application of the magnetic field. If the magnetic field is rotated the beams move around with it so that the magnetic field serves both to focus the beams and to direct them to various points on the anode periphery.

For the second type of electrostatic field, i.e., the uniform field, the magnetic field is maintained parallel to the electric vector. On one side of the cathode the potentials are all positive and the beam is formed, but on the other side all of the potentials are negative and the beam is suppressed. Thus this latter combination of fields eliminates one of the two beams. For this case the electrostatic field must be rotated with the magnetic field if the beam is to be turned.

The magnetic field is obtained from a set of coils in a suitable structure surrounding the tube. The rotation of the field is accomplished by the application of two or three phase currents to these coils. Similarly, the application of two or three phase potentials from the same source to the anode elements connected in groups produces the rotating electrostatic field that is necessary for the single-beam field arrangement. For applications where the beams are not rotated continuously, a two-phase coil arrangement may be used in which the currents through the two windings are adjusted to be proportional to the sine and cosine of the desired direction angle of the beam. Permanent magnets of horseshoe shape are also suitable for use with the tube.

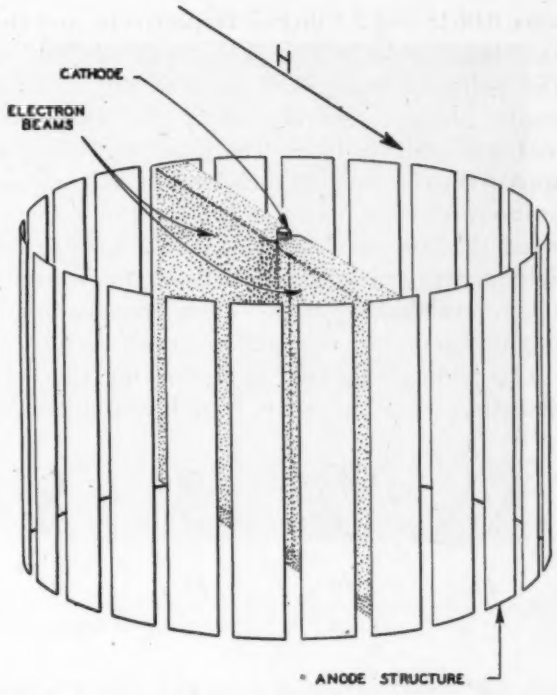

FIG. 1. Elementary tube structure showing focused beams.

Some of the smaller tubes produce beam currents of more than 5 milliamperes with only 50 volts on the anode structure and in some of the tubes with larger cathodes beam currents of 50 milliamperes or more are easily obtainable with a few hundred volts. The magnetic field strengths range from 50 to 300 gausses.

CYLINDRICAL ELECTRICAL FIELD

For the case of the cylindrical electric field the focus is obtained by applying a magnetic field that is strong enough to reduce the radius of curvature of the spiral electron trajectories to a small value. There is not obtained an electron optical image of the cathode in the usual sense that for each point on the cathode there is a corresponding point on the image. The sharpness of the image may be increased by increasing the strength of the magnetic field and the field required for any degree of focus is not sharply critical.

Figure 2 shows a series of drawings of the various electron images that were obtained as the magnetic field strength was increased in a tube having a fluorescent coating on the inside of the anode cylinder. The cathode and anode diameters

were 0.0625 and 2.5 inches, respectively, and the axial length was 2 inches. The anode was held at 150 volts. Only one-half inch of the cathode length, located centrally along the axis, was coated to emit electrons. The image at 340 gauss appeared to be one-half inch long. In attempting to interpret these patterns it should be remembered that on the two sides of the cathode at right angles to the plane of the beam the electrons follow cycloid-like paths along the cathode, moving up on one side and down on the other.

The photographs of Fig. 3 showing the trajectories were obtained by introducing argon at

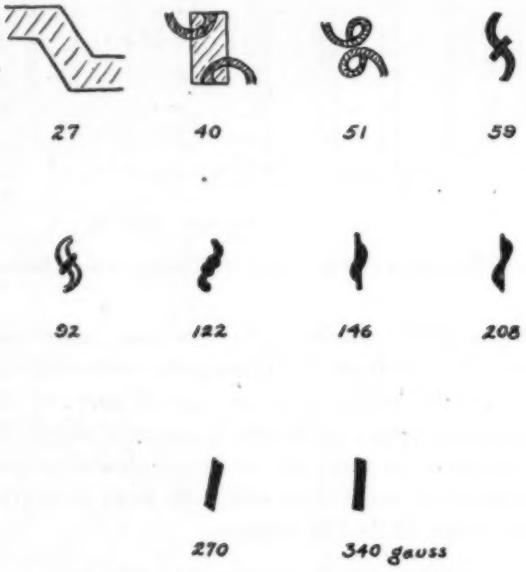

FIG. 2. Drawings of the patterns obtained with a fluorescent coating on the inside of the anode when the magnetic field strength is increased from zero to the focus values.

a pressure of about a micron into the tube. The electrons are emitted from only two spots of active material located at the opposite ends of a diameter on the cathode sleeve. In Fig. 3a the line joining the spots is lined up with the magnetic field and in 3b this line is at an angle of about 45° with respect to the field. This arrangement does not reproduce exactly the space charge conditions in the tube as actually used but does serve to give a picture of the electron paths in a qualitative sort of way.

As shown by the patterns of Fig. 2, above a minimum strength of magnetic field the shape of the focus does not change greatly. An approximate equation may be derived for the beam width in terms of the magnetic field above this minimum value that is useful for predicting the performance of new designs. The electrons that leave the cathode at right angles to the beam require the strongest magnetic field to keep them in focus. Now because of the cylindrical structure, the electric field is concentrated near the cathode and we will assume that after leaving the vicinity of the cathode the velocity does not change appreciably. Setting v equal to the component of this velocity at right angles to the magnetic field we have that the radius r of the spiral path is given by the relation

$$r = mv/eH,$$

where H is the magnetic field strength and m and e are the mass and charge of an electron.

We also write

$$v = (2eKV/m)^{\frac{1}{2}},$$

where K is the fraction of the anode voltage corresponding to v.

The width of the focus A is approximately equal to the cathode diameter D plus twice the maximum radius of curvature of the spiral paths obtained from the above formulae.

$$A \doteq D + [6.7(KV)^{\frac{1}{2}}/H],$$

where A and D are in centimeters and V is in practical volts. By substitution in this formula we have found that the empirical constant K is about 0.7 for the tubes that have been made to date. A minimum value for H is obtained, again approximately, by setting the last term in the equation equal to D.

UNIFORM ELECTRIC FIELD

For the case of the uniform electric field a real electron optical image of the cathode is obtained.

Neglecting the distortion of the field in the vicinity of the cathode, the force equation for the electrons is

$$m(d^2x/dt^2) = e(V/R),$$

where V is the maximum anode potential, R is the radius of the anode structure, and x is measured in the direction of the fields. Since the acceleration is uniform, the transit time t, neglecting space charge effects, may be obtained

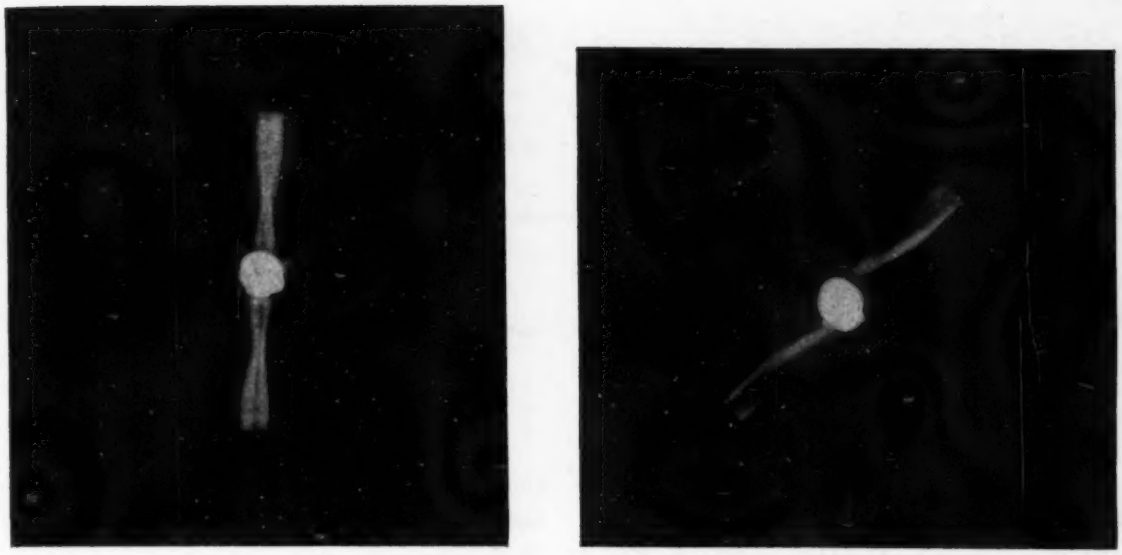

a b

FIG. 3. Electron trajectories made visible with a small amount of gas. (a) Magnetic field lined up with active spots on the cathode. (b) Magnetic field at 45° with respect to the active spots.

from the expression

$$\tfrac{1}{2}[(d^2x)/(dt^2)]t^2 = R.$$

Combining these equations, we get

$$t = R/(Ve/2m)^{\frac{1}{2}}.$$

The condition for focus is that the electrons make one revolution around the lines of force in time t. The angular velocity of the electrons is given by the well-known expression

$$\omega = He/m.$$

Setting $\omega t = 2\pi$, we get

$$H = \frac{2\pi}{R}(mV/2e)^{\frac{1}{2}},$$

or in practical units

$$H = \frac{10.6\sqrt{V}}{R}.$$

Since the effect of the magnetic field on the space charge has not been evaluated, we can only estimate the order of magnitude of the increase of transit time due to the space charge. On the assumption that this increase introduces a factor of $\frac{3}{2}$,* the above expression with space charge is

$$H = \frac{7.1\sqrt{V}}{R}.$$

* The factor of $\frac{3}{2}$ is the ratio of the transit times in a plane parallel diode with and without space charge.

This formula has been found to check well experimentally.

These last two formulae are for the first focus. Focii will also be obtained for values of H equal to nH, where n is an integer and equal to the number of electronic revolutions. Actually as the field is

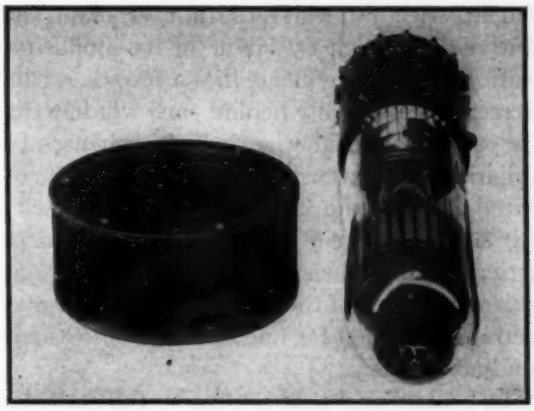

FIG. 4. Radial beam tube with 30 anodes and unwound stator used with it. Small polyphase synchronous motor stators have been found to provide suitable magnetic fields for use with these tubes.

increased beyond that necessary for the first focus the beam does not get very badly out of focus because the radius of curvature of the spiral path is small and for still higher fields the beam remains in approximate focus for all values of H.

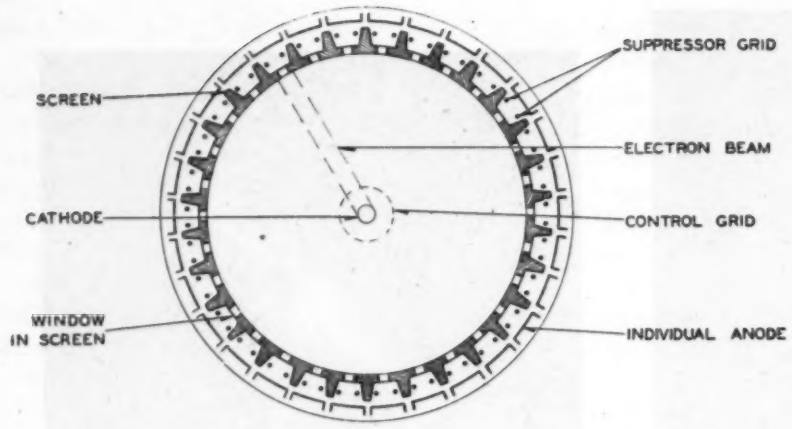

FIG. 5. Arrangement of elements in the tube shown in Fig. 4. Only the operating beam is shown.

TUBE DESIGN

The particular design of tube depends on its application. The simple design shown in Fig. 1 has been found adequate for some purposes but more elaborate designs which increase the versatility of the tube are also needed.

Figure 4 shows a tube with 30 anodes that incorporates various auxiliary elements. This tube is 2.25 inches in diameter. Figure 5 shows the internal arrangement of the elements. Closely surrounding the cathode is a control grid that may be used for modulating the current density of the electron beams. Farther out is a cylindrical element with 30 windows that is maintained positive and which by virtue of its similarity in position to the third element of a tetrode is called a screen. Immediately behind each window there is a pair of paraxial wires which, because of its similarity in function to the fourth element of a pentode, is called a suppressor grid. In back of each suppressor grid there is an anode. In this particular tube there are projections like gear teeth on the back of the screen element to prevent electrons, destined for one anode, from reaching an adjacent one.

The control grid that is close to the cathode is biased negatively and controls the electron current in the same way that it would if the magnetic field were not present. The space current *vs.* grid potential curve is nearly identical for the two cases: with and without the magnetic field. The slight difference is due to the fact that the presence of the magnetic field increases the space charge near the cathode. Thus the tube may be used for amplification in the usual way when the electrons are focused. The presence of this grid has no appreciable effect on the focusing of the electrons.

Since the screen element is in one piece there will be present two beams out to it. One of these may be suppressed after it has passed through the screen by the suppressor grids the manner described below or by the anodes in a similar fashion.

These suppressor grids are generally operated at cathode potential or at a potential that is negative with respect to the cathode. They may be used for three purposes, to suppress secondaries from the anodes, to modulate the beam current to their particular anode, and to suppress one of the two beams. For the first of these functions they are biased at cathode potential. For the second they are biased negatively and have a modulation curve similar to that of the suppressor grid in a pentode. This control is sensitive enough to give amplification of the signals applied to them. Their amplification factor may be increased by welding lateral wires across them. For the third function the screen is maintained at the same positive potential required for the two-beam condition and the suppressors are so biased that they are beyond cut-off on one side of the tube and at or near cathode potential on the other side. If the beam is rotated the suppressors are connected to the polyphase supply in groups in the same way that the screen elements would be connected except that the d.c. bias above and below which the a.c. potentials swing is made negative at a value near cut-off for the suppressors.

The anode characteristics are similar to those of a pentode if suppressor grids are used and to that of a tetrode if these grids are not used.

There is still another method of effectively eliminating one beam. This consists in using an odd number of anodes so that when one beam is focused on an anode the opposite one falls on the screen in between two anode positions. With this type of tube the effective rotational frequency is twice the cyclic frequency of the rotating field, that is, all of the anodes are contacted twice (once for each beam) per revolution of the field.

The many possible combinations of the tube elements just described permit a variety of applications. One of the simplest and most obvious is that of an electronic commutator which has the advantages over the corresponding mechanical device of speed and freedom from contact trouble. A 30-channel time division multiplex system for signaling using two of the 30-anode tubes described above as electronic commutators has been successfully tested* over short distances in the metropolitan area in New York City.

* A. M. Skellett, Bell Sys. Tech. J. **23**, 190 (1944).

Kinematics of Reflection Oscillators*

BY A. E. HARRISON

Sperry Gyroscope Company, Inc., Garden City, New York

(Received June 6, 1944)

ONE of the most interesting differences between velocity modulation tubes and conventional vacuum tubes is the dependence of the current upon a position in space as well as a function of time. An analysis of the problem is simplified if the electron beam is treated as particles; this means that many of the principles of electron optics may be employed. In fact, the term "phase focusing" emphasizes the optical analogy, and was introduced by Bruche and Recknagle[1] to describe the phenomenon which is well known in this country by the term "electron bunching." The basic theory of electron bunching will be reviewed with reference to a double-resonator velocity modulation tube; then the analysis will be extended to an explanation of a Reflex Klystron† oscillator.

An example of one type of double-resonator Klystron is shown in Fig. 1; this tube is a figure of revolution about the axis. If there is no alternating field between the buncher grids, the electron beam is a direct current and the tube is a simple electron gun structure. A radiofrequency field in the first cavity resonator, or buncher, will modify the velocity of the electrons slightly. It is this velocity modulation which makes the current a function of position as well as time. During the transit time required for the electrons

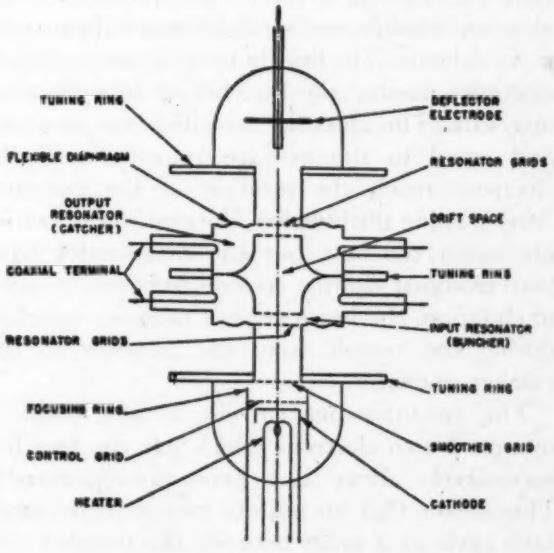

FIG. 1.

* Paper presented at the inaugural meeting of the Division of Electron and Ion Optics of the American Physical Society at Pittsburgh on April 29, 1944.

† Trademarks of the Sperry Gyroscope Company, Incorporated.

to travel from the buncher to the catcher resonator, the faster electrons overtake the slower electrons which left earlier in the cycle. The uniform beam current becomes pulsating or bunched, and part of the energy in the electron

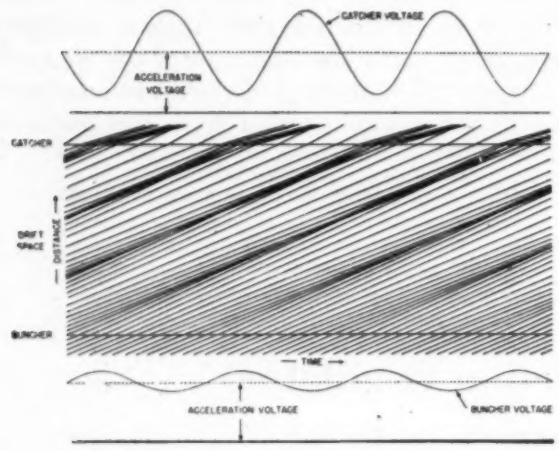

FIG. 2.

beam is converted into radiofrequency energy in the catcher resonator.

These relations can be illustrated with an Applegate diagram as in Fig. 2. A similar diagram for a corrected "phase lens" appeared in the paper by Bruche and Recknagle.[1] Time is measured along the horizontal axis, and distance along the drift space is plotted as the vertical coordinate. This choice of coordinates means that the slope of a line is proportional to the electron velocity, and straight lines indicate constant velocity. The lines in the diagram represent electrons passing the buncher at uniform time intervals. The electron velocities are identical and equal to the average velocity until the electrons reach the position of the buncher. After passing the buncher, the electron velocities are again constant but the magnitudes have been modified slightly. As a result of this velocity modulation, the beam current becomes bunched during the transit from the buncher to the catcher resonator.

The instantaneous current at any point is infinite if two electrons which left the buncher successively arrive at a point simultaneously. This means that an infinite current exists once each cycle at a point between the buncher and the catcher. Beyond this point the lines diverge. Note that the electron which forms the center of the bunch travels with average velocity and passes the buncher resonator when the field is zero and changing from deceleration to acceleration. There are two infinite current peaks per cycle at the position of the catcher; these infinite peaks correspond to the simultaneous arrival of electrons which left after the electron corresponding to the center of the bunch, and a similar simultaneous arrival of electrons which left earlier but traveled more slowly.

Another form of Klystron known as a Reflex oscillator utilizes a single-cavity resonator as both buncher and catcher. Such a tube is illustrated by Fig. 3. The electron beam is velocity modulated as it passes the resonator grids; the electrons are reflected back through the same grids and become bunched while in the reflector field. The Applegate diagram for such a tube is shown in Fig. 4.

The action of the electrons in a reflection oscillator is analogous to the motion of an object in a gravitational field if space charge effects are neglected and the reflecting field is assumed to be uniform. Under these conditions the electron paths will be parabolas in contrast to the straight lines in the Applegate diagram for the double-resonator Klystron. The diagram is not difficult to construct, however, since all of the

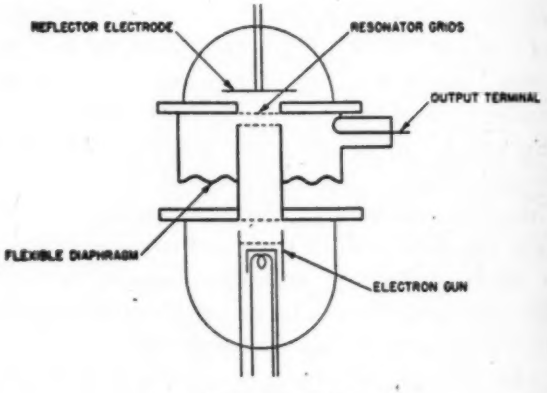

FIG. 3. Reflex Klystron.

electron paths are symmetrical and correspond to different portions of the same parabola.

Electrons which have been speeded up travel farther and take longer than the average time to return to the resonator, and electrons with less than average velocity require less than the

average time. As a result, the bunch in a reflection oscillator is formed around the electron with average velocity which passed the resonator grids when the field was zero and changing from acceleration to deceleration. This behavior is

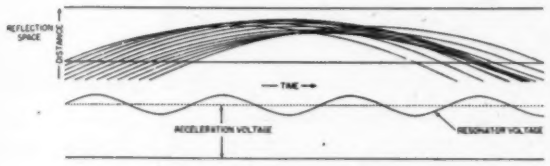

FIG. 4.

the opposite of the action in a double-resonator oscillator, where the bunch was formed about the electrons which passed the buncher grids when the field was changing from deceleration to acceleration. There is a phase difference of 180 degrees between the two types of bunching, but the distribution of current in the bunch is the same in either case although the manner in which the bunches are formed is entirely different.

There are two infinite current peaks in Fig. 4. The first infinite peak corresponds to the simultaneous arrival of electrons which left the resonator after the electron which forms the center of the bunch. The other infinite current peak consists of electrons which left prior to the center of the bunch. Since the faster electrons travel farther and arrive later, there is no crossover of electrons in the diagram for a reflection oscillator, and there is no single infinite current peak formed in the bunching space. This behavior differs from that of a double-resonator tube; the difference is introduced by fact that the transit time is proportional to the reciprocal of the velocity when electrons travel in a field-free space in contrast to a transit time directly proportional to the velocity when bunching occurs in a reflecting field.

Simultaneous arrival of more than one electron does not necessarily imply that the instantaneous current is infinite. The current is not infinite if the electrons which arrive simultaneously leave at radically different times in the cycle. Note that electrons which left the resonator grids when the field was accelerating return at the same time as the electron with average velocity and a decelerated electron. An infinite current exists only when successive electrons arrive simultaneously; in this case the two paths converge slowly as shown by the lines in Fig. 4.

An electric field which accelerates the electrons as they leave the resonator grids will extract energy from the returning bunch. This condition is necessary for oscillation, and examination of the Applegate diagram will show that the average transit time must correspond to $(n-\frac{1}{4})$ cycles if the maximum output is desired. Under these conditions, the electrons in the bunch will be decelerated, and relatively few electrons during the other half of the cycle will absorb energy from the field in the resonator.

If both field-free and reflection bunching occur in different parts of the same tube, the bunching is partially nullified because the two effects are 180 degrees out of phase. The total transit time in both regions determines the phase of the returning bunch with respect to the resonator voltage and governs whether the tube will oscillate, but the effective bunching time is decreased when the two types of bunching occur in the same tube and the equivalent time for bunching considerations is given by the difference between the transit times in the two different regions.

BIBLIOGRAPHY

(1) E. Bruche and A. Recknagle, Zeits. f. Physik **108**, 459–482 (1938).

The Thickness of Electron Microscopic Objects*†

BY ROBLEY C. WILLIAMS AND RALPH W. G. WYCKOFF

Department of Astronomy; and Virus Laboratory, School of Public Health, University of Michigan, Ann Arbor, Michigan

(Received July 17, 1944)

THIS is a preliminary account of experiments made while seeking a way to determine the heights, or thicknesses, of certain objects under the electron microscope. At first, attempts were made to apply the methods of stereoscopic photography to this problem but these were complicated by phenomena presumably due to electron diffraction in the sample. It has been known for some time that effects due to coherently scattered electrons can be recognized under the microscope; our results indicate that at times they are of overwhelming importance in determining the appearance of some crystalline objects. Partly because of these diffraction phenomena it soon became evident that information was needed in our work other than that provided by stereoscopic photography. A procedure for measuring heights based on shadow-casting was accordingly developed to meet this need.

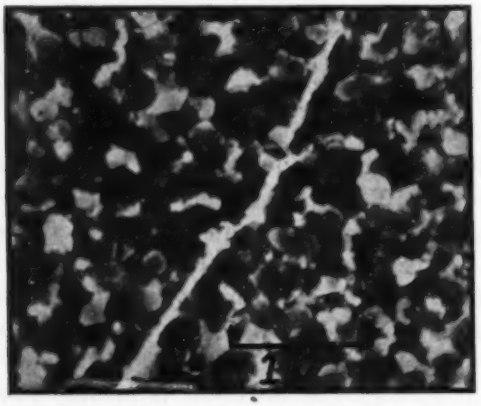

FIG. 1. An electron micrograph made through an evaporated film of metallic bismuth of *ca.* 600A computed thickness. If this film were photographed with the electron beam incident at a different angle (as in a stereoscopic holder) many of the granules which here appear light would undoubtedly be dark, and vica versa. Several of the granules in this picture also show the same kind of light and dark lines, or bands, described by von Ardenne, Hillier and Baker, and others.

Some months ago Picard and Duffendack[1] published in this journal electron micrographs of several evaporated metallic films. Their photographs of aluminum and copper, for example, consist of an unbroken array of mottled areas, some light and others opaque. Extraordinarily fine pictures of this sort, taken through films of silver and of aluminum by Hass,[2] have just come to our attention. Bismuth (Fig. 1) in a computed thickness of about 600A also provides a good example of such a micrograph. Such photographs as these have sometimes been thought to indicate that the films themselves consist of granular aggregates of particles of various thicknesses. Early in our work we made stereoscopic photographs of metallic films and were surprised to find that very different detail appeared on the two members of a stereoscopic pair. This is clearly evident in the stereoscopic photographs of an aluminum film reproduced in Fig. 2. If the large irregular object on the left side of the pictures is used as a point of orientation, study shows that very few of the black dots on one stereogram are to be found on its mate. Films of other metals have yielded similar results though failure to match is not always so complete as in this case.

The work that has been done indicates that in general thin metallic films are of three sorts: (1) continuous, with no indication of structure, like chromium, uranium and very thin antimony; (2) continuous, but a mosaic of light and dark patches, like the bismuth and aluminum films of Figs. 1 and 2; (3) a discontinuous assembly of more or less globular-appearing particles, like indium (Fig. 3). Some metals form films of each type depending on thickness and conditions of deposition. As would perhaps be expected, neither member of a stereoscopic pair of photographs of a continuous chromium film shows any

* Paper presented at inaugural meeting of the Division of Electron and Ion Optics of the American Physical Society at Pittsburgh on April 29, 1944.

† Aided in part by a grant from the National Foundation for Infantile Paralysis, Inc.

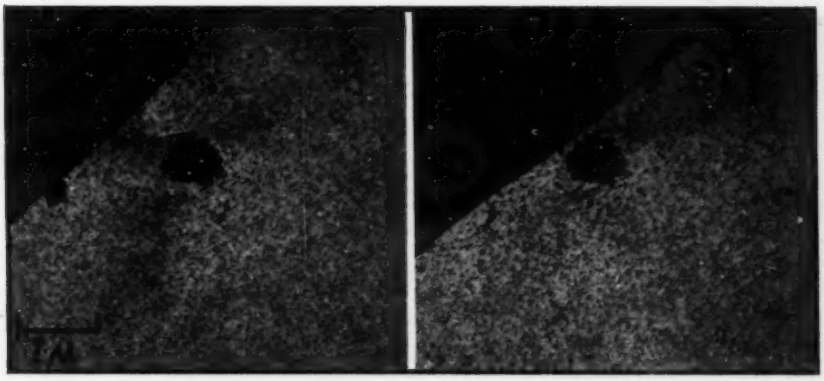

FIG. 2. A stereoscopic pair of electron micrographs of an aluminum film *ca.* 200A thick. The opaque region at the upper left, and the black greatly displaced object on the edge of this opacity, are parts of a wire of the supporting grid (and hence far from the plane of the rest of the preparation). Very few of the dark grains on one photograph appear on the other.

detail whatsoever. Photographs of thin indium (Fig. 3) or of thin bismuth show the same detail on both members of a pair. In such micrographs the individual metallic particles stand out distinctly, but their opacity is not necessarily proportional to their size. The larger particles of thicker films frequently display internal details which are different on the two members of a stereoscopic pair of photographs, and when the film has become so thick as to be substantially continuous it commonly gives a mottled picture like Fig. 1 with features that depend on how the specimen is oriented towards the electron beam.

Much work has been done by electron diffraction on thin metallic films.[3] Comparison with these results makes it clear that the films with which we have dealt were crystalline. Without doubt, therefore, the phenomena causing failure to match are due to electron diffraction within the sample. von Ardenne,[4] Heidenreich,[5] Hillier and Baker,[6] Hass,[2] Kinder,[7] and others have described effects on electron micrographs due to such diffraction. They are important to all phases of electron micrography since because of them the apparent opacity of an object under the microscope is not necessarily an index of its thickness. These effects have been of various sorts and have influenced in varying degrees what is seen under the electron microscope. Heidenreich,[5] for instance, has observed on upturned crystals of MgO a series of light and dark bands which appear to be due to multiple reflections of the incident electrons, alternately out of and then back into the path of direct transmission. Kossel[8] has offered a compatible interpretation of similar photographs by Kinder.[7] Hillier and Baker's[6] experiments showed several black and white lines whose sequence and position varied with the orientation of the sample. Similar sets of lines can be seen on other published photographs,[1,4] notably Hass'[2] picture of a silver film. His photographs, however, like ours indicate that diffraction effects are not limited to such striations but can cover wide areas. It is evident from our stereoscopic photographs that, especially with some crystalline films, so much radiation may be diffracted that it, rather than the non-coherently scattered electrons, will determine the resulting picture. How completely the appearance of an object under the electron microscope may depend on

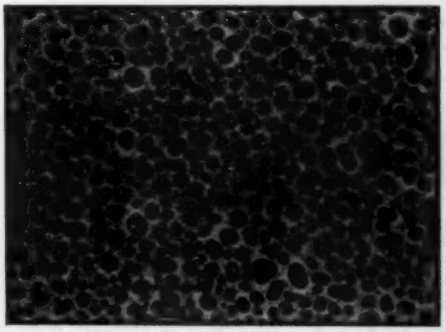

FIG. 3. A photograph through an indium film *ca.* 300A thick. A bismuth film of similar thickness would look almost exactly like this. Here the smallest globules and the big granules appear about equally opaque.

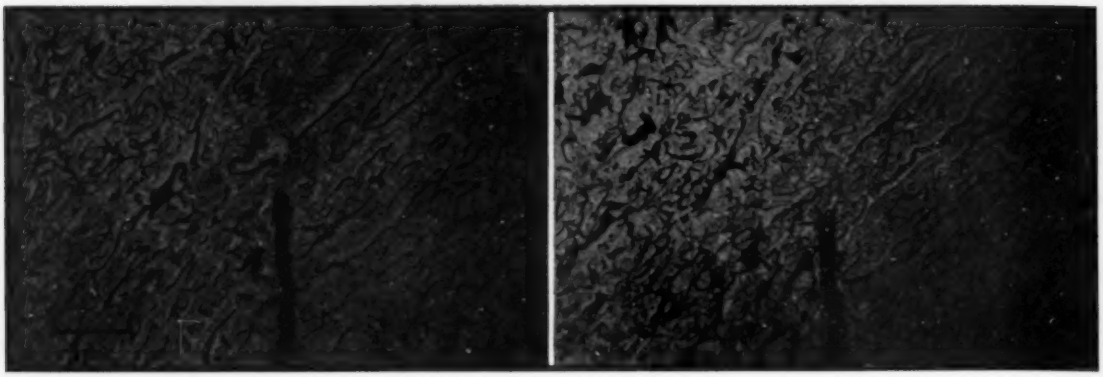

FIG. 4. A stereoscopic pair of electron micrographs made through a film of antimony about 200A thick. Similar regions on the two photographs can be identified by reference to the elongated foreign object in the bottom middle of the field. Successive pictures have been made after an interval of time and after exposure of the film to the air to ensure that the different appearance of these photographs does not arise from changes in the film itself while the experiment was being made.

diffraction is well illustrated by photographs of antimony films. The pair of Fig. 4 was made through a moderately thin antimony film; entirely different regions of darkness, due presumably to the fact that each tilt of the specimen brings different crystalline areas into position for a coherent reflection of electrons away from the transmitted beam, are seen on the two photographs. Even greater difference is shown by the pair of Fig. 5, prepared from a thicker film of antimony; here one knows he is looking at the same field only because identifying holes can be found in the two horizontal cracks across the lower part of the pictures.

It is evident that this dependence of electron microscopic appearance on specimen orientation cannot always be recognized or fully evaluated by studying a single photograph; it is equally clear that other sorts of crystalline materials than metallic films will show these effects. As a result of our experience we would hesitate to interpret in terms of thickness or density any detail on an electron micrograph without studying photographs made at more than one angle of tilt.

The unsatisfactory nature of stereoscopic observation as a way of measuring the heights of certain electron microscopic objects leads us to propose another method based on shadow-casting. It consists essentially of depositing a thin metallic film obliquely onto the preparation in question and then photographing and measuring the lengths of the shadowed areas thus formed on the preparation. There has just come to our attention a paper by Müller[9] who describes a similar shadow technique. Our procedure differs from his in two respects: (1) in the choice of a metal for evaporation that will yield a very homogeneous film, will show no tendency to migrate over the substrate, and thus will yield sharp, clearly-defined shadows; and (2) in casting two shadows simultaneously from directions about 180° apart (Fig. 6). The experi-

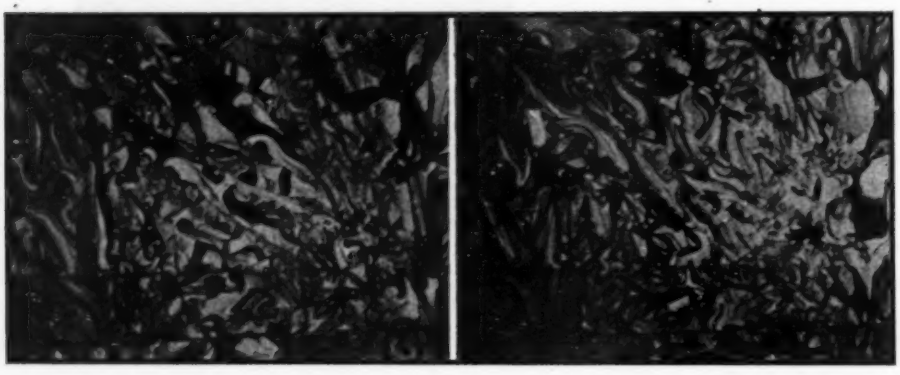

FIG. 5. A stereoscopic pair of micrographs through a thicker antimony film (computed thickness *ca.* 400A).

FIG. 6. Photographs of the shadows obtained when thin films of chromium are evaporated from opposite directions onto a collodion film supporting certain biological objects. The two filaments from which evaporation took place were at different heights above the preparation so that one set of shadows is always longer than the other.

mental arrangement needed for shadow-casting is the simple one, familiar to all who have worked with evaporated films, shown diagrammatically in Fig. 7. Metal from two hot filaments is evaporated simultaneously, or successively, at known angles onto the specimen suitably mounted in the middle of an evacuated bell jar. Two opposite shadows are required since the specimen on its screen is often not horizontal and this will of course greatly alter the lengths of the individual shadows. A sufficient accuracy will, however, result by using the average length of opposed shadows. It is obvious that this method cannot be applied to objects so shaped or situated that they do not cast shadows and that it has only a limited accuracy for many irregularly shaped objects—but for all recognizable objects it can set an upper limit to the height and for many that do cast shadows it sets both an upper and a lower limit. It is practical to work with shadows cast at angles such that the length of shadow is five to ten times the height of the object. Chromium and uranium are useful as shadow-casting metals since both deposit in uniform, structureless films. Uranium will cast perceptible shadows in computed thicknesses of only 5–10A; with chromium about 50A films are needed. As yet we do not know the minimum height that can be measured in this way but we have seen sharp little shadows (Fig. 8) whose lengths indicate that the objects responsible for them were not more than *ca.* 30A high. This is definitely less than the resolving power of the microscope under the conditions prevailing when this picture was made. Evidently shadow-casting can be used for two purposes: (a) to estimate the heights of objects seen under the microscope and (b) to extend still further the limits of our observation giving some idea of the existence and conformation of things below the resolving power of the microscope. Since shadow-casting makes it possible to estimate thicknesses in the

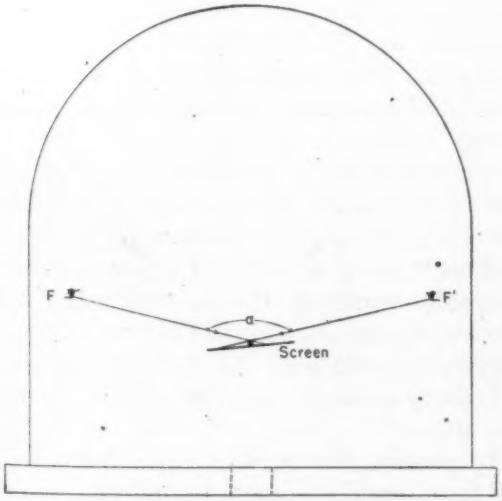

FIG. 7. A schematic drawing of apparatus for shadow-casting onto electron microscopic preparations. The dark object shown in the center of the screen protects portions of the screen from atoms evaporating from filaments *F* and *F'*, and thus creates regions that appear like shadows.

FIG. 8. Another example of a shadow-cast electron micrograph for the determination of the heights of objects. Close inspection of the picture shows minute, sharp shadows down to the limit of visibility to the eye. Shadows cast here are seven times as long as the objects are high. It is to be noticed that in this, and in Fig. 6, the shadow-casting technique brings out much detail of the structure of the supporting collodion films.

range of molecular dimensions, it opens up an interesting field of experiment.

BIBLIOGRAPHY

(1) R. G. Picard and O. S. Duffendack, J. App. Phys. **14**, 291 (1943).
(2) G. Hass, Kolloid Zeits. **100**, 230 (1942).
(3) G. P. Thomson and W. Cochrane, *Theory and Practise of Electron Diffraction* (The Macmillan Company, London, 1939).
(4) M. von Ardenne, Zeits f. Physik 116, 736 (1940).
(5) R. D. Heidenreich, Phys. Rev. **62**, 291 (1942).
(6) J. Hillier and R. F. Baker, Phys. Rev. **61**, 722 (1942).
(7) E. Kinder, Naturwiss. **31**, 149 (1943).
(8) W. Kossel, Naturwiss. **31**, 323 (1943).

Potential Nuclear Monokinetic Electron Sources*

M. L. POOL

Ohio State University, Columbus, Ohio

(Received July 19, 1944)

In this paper sixty-eight nuclear monokinetic electron sources are tabulated. These sources are obtained by producing designated artificial radioactive elements. The voltage of the electrons emitted in the lowest energy group is 17 kev and that in the highest is 578 kev. Applications seem possible in special radio tubes and for certain experiments with electron microscopes and electron diffraction.

AMONG the some 300 synthesized or artificial radioactive nuclei discovered to date, a few have been found which emit electrons in a narrow energy range. Most nuclei, however, emit the well-known and characteristic continuous beta-ray spectrum of electrons or positrons or both.

A summary of the available nuclei capable of emitting monokinetic electrons is given in Table I. The next-to-the-last column lists the energy of the emitted electrons in kilovolts in the order of increasing energy. As may be seen the lowest energy group of electrons, No. 1 of the first column, comes from tungsten of atomic mass number 187. The highest energy group, No. 68, comes from tellurium of atomic mass number 122 or 124. The half-life of this emitting nucleus is 125 days. The minimum and maximum energies are, respectively, 17 and 578 kilovolts.

In most cases only a rudimentary knowledge is available about the monokinetic sources. In a few cases, however, a reasonable amount of detailed work has been reported by the use of a beta-ray spectrometer[15] or spectrograph.[2] In these instances two monokinetic groups are observed, one which is associated with the K-electron shell of the atom and another which is associated with the L-electron shell. The group associated with the K-electron shell is in general the stronger by a factor of eight times. The factor, nevertheless, varies considerably from element to element; for No. 20 the two groups seem to be of equal intensity. In Table I only the monokinetic groups associated with the K-electron shell are listed in the next to the last column.

For a given element the energy difference between the two emitting groups is equal to the energy of the $K\alpha$ x-ray line of the element. This value varies from 3.7 kilovolts for No. 55 to 91 kilovolts for No. 19. Sometimes an electron group has been found which can be identified with the L series, but in every case the intensity is very weak.

Contributions to the theoretical significance and interpretation of the origin of monokinetic electron groups have been made by a number of authors.[4,5] The probability of a gamma-ray being internally converted, the magnitude of the K to L conversion ratio, and the function relating the conversion ratio with the half-life periods and the energy states of nuclei are still in the formative stages.

To predict that nuclear monokinetic sources will be of practical importance in the near future is, at present, without adequate foundation. The state of development is now remindful of that of the Edison effect in 1883. There are a few nuclear sources which even now can be made to

* Paper presented at the inaugural meeting of the Division of Electron and Ion Optics of the American Physical Society at Pittsburgh on April 29, 1944.

furnish currents of the order of 10^{-8} ampere. These could possibly be utilized in certain electron microscope experiments, electron diffraction experiments, and special radio tubes. With the availability of larger cyclotrons, more intense monokinetic sources could be produced and the scope of appliability would be correspondingly enlarged.

TABLE I. Summary of nuclear monokinetic electron sources, listed in the order of increasing voltage of emitted electrons. D, H, M, S represent, respectively, days, hours, minutes, and seconds. The superscripts in column two are the mass numbers of the elements involved.

No.	Nucleus responsible for electron source	Half-life of radioactive nucleus	Energy of gamma-ray internally converted	Voltage of monokinetic electrons emitted by nucleus	References
1	W^{187}	1.0 D	86 kilovolts	17 kilovolts	1
2	Br^{80}	4.4 H	45	23	2, 3, 4
3	W^{187}	1.0 D	101	32	1
4	Br^{78}	6.7 M	46	33	2, 5
5	Kr^{83}	1.9 H	49	35	6
6	As	100 D	52	40	7
7	Re	54 D	113	42	1
8	Ga^{70}	18.5 M	54	44	2
9	Br^{80}	4.4 H	49	47	2, 3, 4
10	I^{131}	8.0 D	80	47	8
11	Hg^{197}	23 H	130	47	9, 10, 11, 12
12	$Te^{122,124}$	30 D	82	50	13, 14
13	$Te^{122,124}$	30 D	88	56	13, 14
14	Sn^{113}	105 D	85	56	15, 16
15	Rh^{105}	4.4 M	80	57	17, 18
16	Re	54 D	129	58	1
17	$Cd^{107,109}$	158 D	86	59	19
18	Hg^{197}	2.7 D	75	61	10, 11, 12
19	Pa^{233}	27.4 D	175	63	20
20	$Cd^{107,109}$	6.7 H	93	66	2, 19, 21, 22
21	W^{187}	1.0 D	135	66	1
22	Ma	91 D	87	66	23, 24
23	In^{113}	17.5 M	95	67	25
24	Te^{129}	32 D	100	68	26
25	Pa^{233}	27.4 D	189	77	20
26	Hg^{197}	23 H	161	78	9, 10, 11, 12
27	Co^{57}	270 D	117	81	27
28	Ga^{67}	3.4 D	100	82	2, 28
29	$Se^{79,81}$	57 M	98	85	6
30	Xe	75 S	125	91	29
31	In^{115}	16.5 M	120	92	25
32	Te^{127}	90 D	125	93	26
33	Co^{57}	270 D	130	94	27
34	Br^{78}	6.7 M	108	105	2
35	Ga^{70}	18.5 M	117	107	2
36	Ma	6 H	129	108	23, 24
37	Cb^{93}	55 D	129	110	30
38	Kr	55 S	127	113	29
39	In^{111}	23 M	160	132	15
40	Te^{131}	1.2 D	165	133	26
41	Xe	75 S	175	140	29
42	In^{112}	2.7 D	173	145	15
43	Sr^{85}	1.2 H	176	160	31
44	Ma	91 D	184	163	23, 24
45	In^{114}	50 D	192	164	15
46	Kr	13 S	187	175	29
47	Pb^{205}	52 H	270	185	32, 33
48	Pa^{233}	27.4 D	304	192	20
49	$Te^{122,124}$	125 D	230	198	34
50	In^{112}	2.7 D	247	219	15
51	Ba	1.6 D	276	239	35
52	Au	3 D	331	250	36
53	Ba^{135}	1.2 D	297	260	23, 24, 37
54	$Au^{196,197}$	5.6 D	356	275	38
55	Sc^{44}	2.4 D	280	280	39, 40
56	Se^{75}	160 D	300	287	41
57	Pa^{233}	27.4 D	405	293	20
58	In^{114}	4.5 H	338	310	15
59	Au^{198}	3 D	410	329	27, 38
60	I^{131}	8 D	367	334	8
61	Y^{87}	3.3 D	370	360	31
62	Sr^{87}	2.7 D	370	360	31, 42
63	In^{113}	1.7 H	390	361	15, 16
64	Hg^{201}	43 M	540	457	10, 11, 43
65	Zn^{69}	13.8 H	470	460	44
66	$Tl^{200,201}$	10.5 H	556	470	43
67	Pb^{205}	2.2 D	588	500	43
68	$Te^{122,124}$	125 D	610	578	34

REFERENCES

(1) G. E. Valley, Phys. Rev. **59**, 686 (1941).
(2) G. E. Valley and R. L. McCreary, Phys. Rev. **56**, 863 (1939).
(3) G. E. Valley and R. L. McCreary, Phys. Rev. **55**, 666 (1939).
(4) L. I. Roussinow and A. A. Yusephovich, J. Phys. U. S. S. R. **3**, 281 (1940).
(5) R. E. Siday, Proc. Roy. Soc. **178**, 189 (1941).
(6) Alexander Langsdorf, Jr., and Emilio Segrè, Phys. Rev. **57**, 105 (1940).
(7) L. G. Elliott and M. Deutsch, Phys. Rev. **63**, 457 (1943).
(8) J. R. Downing, M. Deutsch, and A. Roberts, Phys. Rev. **61**, 686 (1942).
(9) G. E. Valley, Phys. Rev. **60**, 167 (1941).
(10) C. S. Wu and G. Friedlander, Phys. Rev. **60**, 747 (1941).
(11) Gerhart Friedlander and Chien-Shiung Wu, Phys. Rev. **63**, 227 (1943).
(12) A. C. Helmholz, Phys. Rev. **61**, 204 (1942).
(13) E. B. Hales and E. B. Jordan, Phys. Rev. **62**, 553 (1942).
(14) C. V. Kent and J. M. Cork, Phys. Rev. **62**, 297 (1942).
(15) J. L. Lawson and J. M. Cork, Phys. Rev. **57**, 982 (1940).
(16) S. W. Barnes, Phys. Rev. **56**, 414 (1939).
(17) Bruno Pontecorvo, Phys. Rev. **54**, 542 (1938).
(18) G. J. Sizoo and L. F. C. Friele, Physica **10**, 57 (1943).
(19) A. C. Helmholz, Phys. Rev. **60**, 160 (1941).
(20) Edith Haggstrom, Phys. Rev. **62**, 144 (1942).
(21) R. G. Sachs, Phys. Rev. **57**, 159 (1940).
(22) Luis W. Alvarez, A. C. Helmholz, and Eldred Nelson, Phys. Rev. **57**, 660 (1940).
(23) D. C. Kalbfell, Phys. Rev. **55**, 422 (1939).
(24) D. C. Kalbfell, Phys. Rev. **54**, 543 (1938).
(25) R. N. Smith, Phys. Rev. **61**, 389 (1942).
(26) G. T. Seaborg, J. J. Livingood, and J. W. Kennedy, Phys. Rev. **57**, 363 (1940).
(27) E. H. Plesset, Phys. Rev. **62**, 181 (1942).
(28) Luis W. Alvarez, Phys. Rev. **54**, 486 (1938).
(29) E. C. Creutz, L. A. Delsasso, R. B. Sutton, M. G. White, and W. H. Barkas, Phys. Rev. **58**, 481 (1940).
(30) William N. Moquin and M. L. Pool, Phys. Rev. **65**, 60 (1944).
(31) L. A. DuBridge and John Marshall, Phys. Rev. **58**, 7 (1940).
(32) Arthur L. Lutz, M. L. Pool, and J. D. Kurbatov, Phys. Rev. **65**, 61 (1944).
(33) Kasimir Fajans and Adolf F. Voigt, Phys. Rev. **60**, 619 (1941).
(34) E. B. Hales and E. B. Jordan, Phys. Rev. **64**, 202 (1943).
(35) J. M. Cork and Gail P. Smith, Phys. Rev. **60**, 480 (1941).
(36) J. L. Lawson and J. M. Cork, Phys. Rev. **58**, 580 (1940).
(37) Katherine E. Weimer, M. L. Pool, and J. D. Kurbatov, Phys. Rev. **59**, 63 (1943).
(38) B. Pontecorvo, Nature **144**, 212 (1939).
(39) Harold Walke, Phys. Rev. **57**, 163 (1940).
(40) Carl T. Hibdon, M. L. Pool, and J. D. Kurbatov, Phys. Rev. **63**, 462 (1943).
(41) C. V. Kent, J. M. Cork, and W. G. Wadey, Phys. Rev. **61**, 389 (1942).
(42) L. A. DuBridge and John Marshall, Phys. Rev. **56**, 706 (1939).
(43) R. S. Kirshnan and E. A. Nahum, Proc. Camb. Phil. Soc. **36**, 490 (1940).
(44) J. W. Kennedy, G. T. Seaborg, and E. Segrè, Phys. Rev. **56**, 1095 (1939).
(45) M. H. Hebb and Eldred Nelson, Phys. Rev. **58**, 486 (1940); S. M. Dancoff and P. Morrison, Phys. Rev. **55**, 121 (1939).

Here and There

Staff Changes

The Department of Physics of the University of California at Los Angeles announces the following changes: Professor S. J. Barnett has retired with the title Emeritus. He will continue his work on gyromagnetism at the California Institute of Technology. Professor V. O. Knudsen, Dean of the Graduate Division, has returned after nearly three years spent with the National Defense Research Committee. Dr. J. W. Ellis has been promoted to a full professorship of physics and has been appointed Chairman of the department. Professor Joseph Kaplan is serving as Chief of Operations Analysis, Second Army Air Force. Assistant Professor A. H. Warner has been promoted by the Army to the rank of Colonel, and is serving in England with the Supreme Command, A.E.F. Dr. L. P. Delsasso, Lieutenant Commander, USNR, has been promoted to an assistant professorship but is serving with the U. S. Navy Radio and Sound Laboratory in San Diego, California. To serve in the absence of regular members of the staff, Professor James A. Swindler, Head of the Department of Physics of Westminster College, New Wilmington, Pennsylvania, has become an assistant professor. The work in meteorology, heretofore done within the Department of Physics, has now been taken over by the newly established Department of Meterorology, of which Professor Jakob Bjerknes is Chairman.

At the annual general meeting of the British Physical Society held on May 24, the following officers were elected: President, Professor E. N. da C. Andrade; Vice President, Sir Edward Appleton; Honorary Secretaries, J. H. Awbery (Papers) and Dr. W. Jevons (Business); Honorary Treasurer, Dr. C. C. Paterson; new Members of Council, Professor S. Chapman, C. H. Collie, and Professor H. R. Robinson. At an extraordinary general meeting held on the same day, A. F. Joffe was elected an honorary fellow.

At the University of London, Dr. Frank Horton, Professor of Physics, has been re-elected Vice Chancellor. Dr. H. T. Flint, reader in physics at King's College, has been appointed to the Hildred Carlile Chair of Physics tenable at Bedford College.

The retirement is announced of Dr. William F. Steve, Professor of Physics at the University of Wisconsin, with which he has been connected for thirty-seven years.

Dr. Harvey A. Zinszer, since 1929 Head of the Department of Physics and Astronomy at the Kansas State College at Fort Hays, has been granted indefinite leave of absence to accept a war defense position in the Cruft Laboratory of Harvard University.

Dr. Maurice Ewing, now engaged in research for the NDRC with the civilian rank of "chief scientist," has been appointed Associate Professor of Geophysics in the Department of Geology of Columbia University. He will direct graduate instruction in geophysics as part of a postwar program of geological training and research. He also plans to continue his investigations of the continental shelf and the ocean basins.

Dr. Homer L. Dodge, Professor of Physics at the University of Oklahoma, Dean of the Graduate School, and Director of the University of Oklahoma Research Institute, has been elected the eighteenth President of Norwich University, Northfield, Vermont. Since 1942 Dr. Dodge has been on leave of absence to serve as Director of the Office of Scientific Personnel of the National Research Council. He assumed his duties as President on August 1. Norwich University is a military college with basic curricula in liberal arts and engineering. The one hundred and twenty-fifth anniversary of its founding was celebrated on August 6 with Colonel Herman Beukema, formerly Director of the Army Specialized Training Program and now of the U. S. Military Academy at West Point, as the principal speaker.

Glenn C. Henry, formerly Chief of the Audio and Industrial Section of the Radio and Radar Division of the War Production Board, has been appointed to the staff of the Sound Equipment Section of the Radio Corporation of America, in charge of sales of engineered sound systems and components. Nearly ten years ago, Mr. Henry entered federal government service in Washington, D. C., serving for seven years as engineer on sound recording and reproduction for the National Archives before he became associated with WPB.

Littlefuse, Incorporated of Chicago and El Monte, California, announces the appointment of R. G. Akin as Sales Manager, Midwest Division of Littlefuse, Inc. Preceding this connection, he was national Sales Manager of the cellulose tubing division of Sylvania Industrial Corporation, New York.

The Sharples Corporation of Philadelphia is expanding considerably its research activities. Dr. Foster C. Nix, physicist, formerly with the Bell Telephone Laboratories, is Director of Research and is engaged in building up his staff. Among those who have recently joined the new organization are: Dr. Robert E. Barieau, Ph.D. from the University of California, 1940; Dr. Walter J. Moore, Ph.D. from Princeton University, 1940; and Dr. Donald W. Collier, Ph.D. from Princeton University, 1944. It is understood that a new laboratory building will be constructed in the Philadelphia area after the war.

It was announced by the Industrial Management Society that the eighth Annual Time and Motion Study Clinic for engineers, executives, and supervisors, will be held November 2 and 3, 1944 at Medinah Club, Chicago, Illinois. Outstanding speakers such as Allan H. Mogenson, Lillian M. Gilbreth, and Ralph M. Barnes are on the program. The Clinic theme will be "More production with less effort."

Necrology

Sir Ralph Fowler, O.B.E., F.R.S., M.A., since 1932 Plummer Professor of Mathematics at the University of Cambridge, died on July 28 at the age of fifty-five years.

Dr. William D. Henderson, physicist, Director of the Extension Division of the University of Michigan, died on May 26 at the age of seventy-seven years.

Dr. J. K. Roberts, physicist, Fellow of Christ's College, Cambridge, died on April 25 at the age of forty-seven years.

Honors and Awards

Lyman James Briggs, Director of the National Bureau of Standards, was awarded the degree of Doctor of Science at the one hundred and ninetieth commencement of Columbia University.

Physicists of Harvard University and of the Massachusetts Institute of Technology on July 9 joined in greeting Dr. Peter Kapitza, Director of the Institute for Physics of the Academy of Sciences of the U.S.S.R., whose fiftieth birthday was being celebrated by the academy in Moscow. Their message offered "hearty congratulations from their American colleagues and sincere wishes for many years of continued fruitful work." Dr. Kapitza has been awarded the Order of Lenin "for outstanding scientific achievements in the sphere of physics."

Dr. Harry Bateman, Professor of Mathematical Physics and Aeronautics at the California Institute of Technology, and Dr. W. M. Whyburn, Professor of Mathematics and Chairman of the department at the University of California at Los Angeles, have been elected corresponding members of the Academia Nacional de Ciencias Exactas, Fisicas y Naturales de Lima.

At the commencement of Harvard University on June 29 the honorary doctorate of science was conferred on Dr. Emory Leon Chaffee, Rumford Professor of Physics and Director of the Cruft Memorial Laboratory of the University.

The Lamme Medal for "outstanding engineering achievement" for 1944 has been awarded by the Ohio State University to Henry M. Williams, of Dayton, Ohio, since 1938 Vice President of the National Cash Register Company in charge of engineering and research. The presentation will be made in June during the commencement of the university.

The Board of Directors of The Electrochemical Society, an international organization, announces the award of the eighth Edward Goodrich Acheson Medal and Thousand-Dollar Prize to Dr. William Blum, Chief of the Section of Electrochemistry, U. S. Bureau of Standards. Dr. Blum is in a very large measure responsible for the standardization of electroplating methods and of plating formulas.

Division of Acoustical Research

Rutgers University has announced the organization of a Division of Acoustical Research in the College of Engineering for the purpose of investigating airborne sounds. The work will be done under contract with the Office of Scientific Research and Development and will be directed by Dr. Carl F. Eyring, Professor of Physics, Brigham Young University. Other members of the staff are Arthur A. Allen, Professor of Ornithology, Cornell University; Wayne B. Hales, Professor of Physics, Brigham Young University; James L. Potter, Professor of Electrical Engineering, Rutgers University; Peter P. Kellogg, Assistant Professor of Ornithology, Cornell University; Obed C. Haycock, Associate Professor of Electrical Engineering, University of Utah; and Wm. L. Nastuk, Assistant in Physiology, and Anthony J. Del Mastro, Instructor in Civil Engineering, both of Rutgers University.

New Mathematical Table

Announcement of a new mathematical table obtainable from the National Bureau of Standards, Washington, D. C. was made on July 21, 1944.

MT29. Table of Coefficients for Inverse Interpolation with Advancing Differences.

By Herbert E. Salzer, Mathematical Tables Project, National Bureau of Standards.

This table may be regarded as a companion table to MT27, "Table of coefficients for inverse interpolation with central differences." It contains tables giving values to 10 decimal places for

4th- and 5th-order terms	for	$m=0(0.001)1.000$;
6th-order terms	for	$m=0(0.01)1.00$; and
7th- and 8th-order terms	for	$m=0(0.1)1.0$.

All these values are correct to about half a unit in the tenth decimal place with the exception of the coefficient of $\Delta^2\Delta^2/\Delta\Delta$ which is accurate to within a unit in the tenth decimal place. A condensed one-page table of coefficients of the fourth-, fifth-, and sixth-order terms, at intervals of 0.1, is also given for the sake of convenience.

Coefficients of the second- and third-order terms $m(1-m)/2$ and $m(1-m)(m-2)/6$, respectively, were not tabulated since they are both tabulated at intervals of 0.0001 by the Mathematical Tables Project in the "Tables of Lagrangian interpolation coefficients" published by the Columbia University Press, New York, New York. For m (there "p") ranging from 0 to 1, $m(1-m)/2$ is given by $-A_{-1}$ in the three-point table and $m(1-m)(m-2)/6$ is given by A_{-1} in the four-point table.

(Reprinted from *Journal of Mathematics and Physics*, May, 1944) 28 pages, with cover, 25 cents.

Division of High Polymer Physics

The *Journal of Applied Physics* has been designated by the Division of High Polymer Physics of the American Physical Society as the medium for the publication of its official announcements. Division Secretary Lyons announces that copies of the by-laws of the Division are now available to members on request to his office (Southern Regional Research Laboratory, New Orleans 19, Louisiana).

National Electronics Conference

As reported earlier, a National Electronics Conference is being sponsored by the Illinois Institute of Technology, Northwestern University, the Chicago Section of the Institute of Radio Engineers, and the Chicago Section of the American Institute of Electrical Engineers with the cooperation of the Chicago Technical Societies Council. Conference activities are scheduled for October 5, 6, 7 at the Medinah Club of Chicago.

The program for this Conference has been arranged as follows:

Thursday, October 5

9:00 A.M. Registration
10:00 A.M. General Meeting
12:30 Noon Luncheon Meeting
2:00 P.M.
1. Television
2. Electronic Power Applications
3. Electronic Aids of Medical Science
4. Survey of Industrial Electronics

6:30 P.M. Social Hour
7:30 P.M. Electronics Conference Banquet

Friday, October 6

9:00 A.M.
5. Radio
6. Electronic Measurements and Controls
7. Recent Developments in Theoretical Electronics

12:30 Noon Luncheon Meeting
2:00 P.M.
8. Electron Tube Developments
9. Industrial Applications—Electronic Devices
10. Aeronautical Applications

7:30 P.M.
11. Ultra-High Frequencies
12. High Frequency Heating
13. Industrial Radiography

Saturday, October 7

9:00 A.M.
14. Radio and Telephone Applications
15. Recent Developments in Electron Theory
16. Industrial Applications

New Book

Cellulose and Cellulose Derivatives

BY STAFF OF SPECIALISTS; edited by EMIL OTT. Pp. 1176+xi, Figs. 286, 15×23½ cm. Interscience Publishers, Inc., New York, 1943. Price $15.00.

This encyclopedic volume is the fifth of a series of monographs which is being issued from time to time by Interscience on the chemistry, physics, and technology of high polymeric substances. The book has been organized with the intention of making available a digest of the most advanced knowledge in the field of cellulose and its applications. Indeed, some of the research results appear in print for the first time in this book. The remark in the preface that "the historical approach has been almost entirely neglected" is somewhat misleading, for a 25-page historical survey introduces the chapter on "Chemical nature of cellulose and its derivatives."

Confirming the growing recognition on the part of American physicists of the role being played by their science in high polymer research, about one-quarter of this volume is devoted to physical properties and methods of research. Thus in the chapter on "Structure and properties of cellulose fibers" is a section on x-ray examination by Wayne A. Sisson, which is indubitably the most complete, single account of the application of the x-ray technique to the study of cellulosic fibers yet to appear. Another section by C. W. Hock, H. Mark, and G. R. Sears, in this chapter, deals with observations obtained by two other physical techniques, visual microscopy and electron microscopy. There is, however, no physical theory in the discussion, which is devoted to the fine structure revealed by these methods. Unfortunately, the publication date of the volume permitted only a footnote reference to the electron-microscopic study of Barnes and Burton which brilliantly confirmed the existence in visual microscopy of diffraction effects which had misled some workers into erroneous concepts of the fine structure of cellulose.

Practically all of Chapter IX on "Physical properties of cellulose and its derivatives" will be found of interest to the physicist. This chapter contains articles by H. M. Spurlin, M. L. Huggins, G. H. Pfeiffer, R. H. Osborn, H. Mark, and R. F. Nickerson on the nature of the interaction of cellulosic substances with various solvents; the thermodynamic and viscous properties of the resulting solutions; methods and uses of viscometry; molecular-weight determinations by physical methods; polymolecularity; and the molecular theory and mechanical properties of cellulosic films, fibers, and yarns. Other chapters deal with the occurrence of cellulose in nature; the chemistry of cellulose, its derivatives, and associated substances; the processing of cellulosic materials; and technical applications.

Some overlapping and repetition occur, as they are bound to when numerous authors, with more or less independent approaches, contribute to the writing of a book, without undertaking a long process of rewriting. While this duplication is not serious and, indeed, permits each section to be a self-contained article, it indicates that the volume is not as concise as the term "digest" would imply. Unfortunately, an unexplained discrepancy concerning the name of the "father of cellulose chemistry" has crept into the volume. On pp. 29–30 he is referred to as Jean Baptiste Payen, whereas in the biographical references cited, in those by Reid and Dryden and Phillips the name is Anselme Payen. Mathematical rigor calls for increment, rather than differential, notation in Eqs. (1) and (2), p. 992; in Eq. (1) also, the initial volume V should appear to the first power only. An admirable feature, common to all volumes in this series, is the liberal repetition of footnote references, so that they generally appear in conjunction with that portion of the text in which they are mentioned.

W. JAMES LYONS
Southern Regional Research Laboratory

Contributed Original Research

Limiting Stable Current in Electron Beams in the Presence of Ions*

J. R. PIERCE
Bell Telephone Laboratories, Inc., New York, New York
(Received July 11, 1944)

In electron flow, the net electronic charge may be neutralized by positive ions. In this case, for a given geometry there is a limiting current beyond which homogeneous flow is unstable. This limiting current is evaluated for flow normal to parallel plane equipotentials and for flow filling a conducting tube and constrained to motion parallel to the axis. For parallel planes at a potential V_0 volts and spaced a distance L cm apart, the limiting current density in amperes/cm^2 is $i_0=104\times10^{-6}V_0^{\frac{3}{2}}/L^2$. For a long conducting tube the limiting current is $I_0=160\times10^{-6}V_0^{\frac{3}{2}}$. These limiting currents are roughly 6 times as great as in the absence of ions.

1. INTRODUCTION

IT has been pointed out by several people that when electron flow takes place in a space essentially surrounded by an equipotential surface, one would expect no appreciable potential depression due to the electron flow. If the ions produced are say 20,000 times as heavy as electrons, a potential depression of a very, very small fraction of the electron energy in volts should overcome the velocities they receive in collisions and should prevent their escape. Thus even in a good vacuum one would expect ions to collect in sufficient numbers to neutralize electronic space charge almost completely.

It would seem, then, that in many cases the behavior of electron flow should be analyzed on the assumption of the presence of heavy ions sufficient to neutralize the average charge of the electron flow. This assumption has been used in some cases, apparently purely for the sake of simplicity.[1-3]

The analysis presented here is based on the plasma oscillation equations of Tonks and Langmuir,[4] retaining their assumption of a constant average charge density through the volume considered. For the sake of simplicity, the magnetic field produced by the moving charges has been neglected.

In Tonks and Langmuir's paper, no attempt was made to take boundary conditions into account. The problem of boundary conditions has been ingeniously circumvented by other writers.[1-3] In the work here presented it is necessary to consider boundary conditions. The writer has been particularly interested in electron flow in the presence of ions and the absence of a steady magnetic field. The work in this memorandum treats one-dimensional flow of this sort. In attempting to cope with two-dimensional flow or with axially symmetrical flow, cases of more interest, the writer has been unable to satisfy the boundary conditions. This dilemma deserves further consideration. If it is assumed that the electrons cannot move perpendicular to the direction of flow, as should be the case with an infinitely strong magnetic field parallel to the flow,[1] the boundary conditions can be satisfied. This case is briefly discussed for axial symmetry.

2. CASE OF NO MAGNETIC FIELD

In presenting the simple mathematics involved in the case of no magnetic field, a certain physical insight can be gained by reviewing the case considered by Langmuir and Tonks in which the electrons have no average velocity. Average

* Paper presented at the inaugural meeting of the Division of Electron and Ion Optics of the American Physical Society at Pittsburgh on April 29, 1944.

[1] W. C. Hahn, Gen. Elec. Rev. **42**, 258–270 (1939).
[2] Simon Ramo, Proc. I.R.E. **27**, No. 12 (1939).
[3] Simon Ramo, Phys. Rev. **56**, 276 (1939).
[4] Lewi Tonks and Irving Langmuir, Phys. Rev. **33**, 195–210 (1929). Also see note Phys. Rev. **33**, 990 (1929).

components are denoted by subscripts $_0$ and a.c. components have no subscript. Assume that the average electronic charge ρ_0 is constant throughout the space considered, and that it is neutralized by a rigidly fixed positive charge. According to our assumptions we have Poisson's equation

$$\nabla^2\varphi = -\rho/\epsilon. \tag{1}$$

The equation of continuity

$$\nabla\cdot[(\rho+\rho_0)\bar{v}] = -\partial\rho/\partial t \tag{2}$$

and the force equation

$$d\bar{v}/dt = -\eta\nabla\varphi. \tag{3}$$

M.K.S. units are used. η is the charge to mass ratio of the electrons. The total derivative with respect to time in (3) means following the electron in its path.

Assuming a sinusoidal oscillation of radian frequency ω we may rewrite (2)

$$\bar{v}\cdot\nabla\rho+\rho\nabla\cdot\bar{v}+\rho_0\nabla\cdot\bar{v} = -j\omega\rho. \tag{2a}$$

For small oscillations we may neglect the first two terms, since they represent the product of two a.c. quantities. Thus we obtain

$$\rho_0\nabla\cdot\bar{v} = -j\omega\rho. \tag{2b}$$

We may rewrite (3)

$$\frac{\partial v_x}{\partial x}v_x+\frac{\partial v_x}{\partial y}v_y+\frac{\partial v_x}{\partial z}v_z+j\omega v_x = -\eta\frac{\partial\varphi}{\partial x}, \tag{3a}$$

etc.

Neglecting terms involving products of a.c. quantities, we obtain

$$\bar{v} = (j\eta/\omega)\nabla\varphi. \tag{3b}$$

Combining (3b), (2b), and (1) we obtain

$$\omega^2\nabla^2\varphi = (\eta\rho_0/\epsilon)\nabla^2\varphi. \tag{4}$$

There are two possibilities. Either

$$\nabla^2\varphi = 0 \tag{5}$$

or

$$\omega^2 = \eta\rho_0/\epsilon = \omega_0^2. \tag{6}$$

The first of these solutions is a solution which could exist in the absence of the charge.

The second sort of solution can have a perfectly arbitrary spatial distribution of potential, from which other quantities can be derived. It is also odd in that the current associated with it is zero, the electron convection current just balancing the displacement current. By specifying a traveling sinusoidal spacial distribution in one direction "waves" can be constructed. As the frequency is always given by (6), the phase velocity will depend on the wave-length

$$v_\varphi = \lambda f = \lambda\omega_0/2\pi. \tag{7}$$

The group velocity of these waves is zero, and they carry no energy.[5] These waves ingeniously behave themselves so that a disturbance in an isolated volume produces no effect outside that volume (for instance, note the absence of current crossing any boundary).

Despite the absence of current, these waves are important in analyzing the effect of the charges on an external circuit. For instance, suppose electrons undergoing a disturbance for which there is no current move bodily with an average velocity v_0 into the space between two closely spaced grids. The first grid shields the space between the grids from the electric field of the oscillation and hence from the displacement current. The uneven distribution of charge constituting the a.c. charge density persists, however, and gives rise to an induced current in the circuit between the grids. If the transit time between the grids is short, the induced current is just $(\rho v_0+\rho_0 v)$.

In another case, to be discussed, the fields satisfying (6) are necessarily associated with fields satisfying (5) in satisfying the boundary conditions. Thus the fields satisfying (6) play a part in the effect on the external circuit, even though by themselves they cause no current to flow.

3. ONE-DIMENSIONAL FLOW

As a magnetic field parallel to the direction of electron motion would not affect one-dimensional flow, the material in this section may be regarded as treating the case of moving charges either in the presence or in the absence of a magnetic field.

One way of tackling the problem of moving charges would be to transform solutions for

[5] Lewi Tonks, Phys. Rev. **33**, 239–242 (1929).

fixed charges. It is perhaps less confusing to start afresh with the assumption of a steady velocity v_0 in the x direction and no velocities in the y and z directions. We will refer to the x component of velocity simply as v. Our equations are

$$\nabla^2\varphi=-\rho/\epsilon, \tag{1}$$

$$(\partial/\partial x)[(\rho+\rho_0)(v+v_0)]=-\partial\rho/\partial t, \tag{2d}$$

$$[d(v+v_0)]/dt=-\eta(\partial\varphi/\partial x). \tag{3d}$$

Assuming a sinusoidal oscillation of radian frequency ω and making the same assumption of small signal as before, we obtain

$$\partial^2\varphi/\partial x^2=-\rho/\epsilon, \tag{1a}$$

$$v_0(\partial\rho/\partial x)+\rho_0(\partial v/\partial x)=-j\omega\rho, \tag{2e}$$

$$v_0(\partial v/\partial x)+j\omega v=-\eta(\partial\varphi/\partial x). \tag{3e}$$

The solution for which $\rho=0$ is

$$\varphi=D+Ax. \tag{8}$$

From (2e)

$$\partial v/\partial x=0. \tag{9}$$

And hence from (3e)

$$j\omega v=-\eta A,$$
$$v=(j\eta/\omega)A. \tag{10}$$

For the current

$$I=v\rho_0+\epsilon(\partial/\partial t)(-\partial\varphi/\partial x)$$
$$=j(\rho_0\eta/\omega-\epsilon\omega)A. \tag{11}$$

In order to obtain the "wave" solution for which $\rho\neq0$ but $I=0$, assume a variation with distance as $e^{-j\beta z}$. Rewriting (1a), (2e), and (3e)

$$\beta^2\varphi=\rho/\epsilon, \tag{1b}$$

$$\rho=-\beta\rho_0 v/(\beta v_0-\omega), \tag{2f}$$

$$v=-\beta\eta\varphi/(\beta v_0-\omega). \tag{3f}$$

From (1b), (2f), and (3f)

$$\beta^+=(\omega+\omega_0)/v_0, \tag{12}$$

$$\beta^-=(\omega-\omega_0)/v_0,$$

$$\omega_0^2=\eta\rho_0/\epsilon. \tag{13}$$

Thus the complete solution for the potential may be written

$$\varphi=Ax+Be^{-j\beta^+z}+Ce^{-j\beta^-z}+D. \tag{14}$$

In order to express the result simply we define the following quantities

$$A=K(\omega^2/v_0), \tag{15}$$

$$\omega x/v_0=\theta, \tag{16}$$

$$\omega_0 x/v_0=\theta_0. \tag{17}$$

If we adjust the constants so that at

$$x=0, \quad \varphi=\rho=v=0 \tag{18}$$

we obtain

$$\varphi=K\omega\Big\{\theta+(j/2)(\theta_0/\theta)$$
$$\times\Big[\frac{\theta-\theta_0}{\theta+\theta_0}(\exp[-j(\theta+\theta_0)]-1)$$
$$-\frac{\theta+\theta_0}{\theta-\theta_0}(\exp[-j(\theta-\theta_0)]-1)\Big]\Big\}, \tag{19}$$

$$I=K\omega(j\epsilon v_0/x^2)(\theta_0^2-\theta^2), \tag{20}$$

$$Z=-\varphi/I. \tag{21}$$

The negative sign appears in the expression for Z, the impedance per cm², because of the direction chosen for positive current flow.

Suppose we consider these equations to represent conditions between two parallel grids tied together with zero impedance, and with an electron current injected normal to the grids.

For unforced oscillations to take place in our short-circuited diode, we must have $\varphi=0$ for $x=L$, where L is the distance between the grids. Therefore, we have φ, as given by (19), zero for values of θ and θ_0.

$$\theta=\omega L/v_0 \quad \text{and} \quad \theta_0=\omega_0 L/v_0.$$

This relation determines ω when ω_0 and L/v_0 are specified.

In particular, we find that we can have $\omega=0$ when $\omega_0 L/v_0=\pi$. If we have $\omega_0 L/v_0=\pi+\alpha$, where α is a small quantity, the corresponding value of ω is approximately

$$\omega=-j\pi v_0\alpha/4L. \tag{22}$$

Accordingly, as α is positive or negative, we have, therefore, a current which increases or decreases exponentially with time. Thus π is the limiting value of $\omega_0 L/v_0$, or perhaps we should say a limiting value of $\omega_0 L/v_0$, for stable electron flow.

In terms of current density i_0, and expressing the velocity in terms of a direct potential V_0, $\theta_0=\pi$ becomes

$$i_0=2^{\frac{1}{2}}\pi^2\eta^{\frac{1}{2}}\epsilon(V_0^{\frac{1}{2}}/L^2)$$
$$=104\times10^{-6}(V_0^{\frac{1}{2}}/L^2). \quad (23)$$

Here potential is in volts, current in amperes, and distance in centimeters. For the analogous case without positive space charge to neutralize the electronic space charge, the maximum stable current density is[6,7]

$$i_m=18.6\times10^{-6}(V_0^{\frac{1}{2}}/L^2). \quad (24)$$

Thus, the presence of ions increases the current which can be passed, but not indefinitely.

The oscillation at the critical current is particularly interesting since at $\theta_0=\pi$ and $\theta=0$, the impedance per cm² is not zero but is $4V_0/i_0$. The condition for oscillation in a circuit is that the sum of the impedances looking both ways is zero; hence we would expect that for oscillation in a short-circuited diode (external impedance zero) that Z should be zero. This "oscillation" is of course rather odd in that the frequency is zero. Perhaps we can say that this "oscillation" must be considered as purely electronic; that is, unaffected by the circuit. However, the presence of a finite impedance between the grids may make increasing oscillations possible at currents lower than the limiting current given above, and these might result in the formation of a virtual cathode. Thus in some cases the maximum current in the presence of ions might be about the same as that in the absence of ions, and both currents might be lower than that given by (23). The problem with a finite circuit impedance Z_c is merely that of finding the roots of $Z+Z_c=0$.

So far, the solutions have assumed that the positive charges are fixed, or that the positive charges have infinite mass. This is legitimate except near $\omega=0$. It seems that the conclusions drawn here will not be seriously affected by the fact that the actual positive charges do have finite mass. Although at $\theta_0=\pi$, $\omega=0$, at some larger value of θ_0 an increasing oscillation will exist for which $\omega\neq0$. Thus instability will be encountered for a current near i_0 as expressed by (23).

In addition to the variations of potential with distance which have been noted so far, there will be a small steady potential such as to retain ions or get rid of excess ions. This will be of little importance in the one-dimensional case investigated here, but might be very important in the two-dimensional and axially symmetrical cases because of the focusing it would produce.

4. AXIALLY SYMMETRIC FLOW WITH NO RADIAL MOTION

In treating the case of axially symmetrical flow with no radial motion (infinite axial magnetic field) we can use (2f) and (3f). In place of (1a) we have

$$\frac{\partial^2\varphi}{\partial r^2}+\frac{1}{r}\frac{\partial\varphi}{\partial r}-\beta^2\varphi=-\frac{\rho}{\epsilon}. \quad (25)$$

φ is now regarded as being a function of r.

Combining (22) with (2f) and (3f) we obtain

$$\frac{\partial^2\varphi}{\partial r^2}+\frac{1}{r}\frac{\partial\varphi}{\partial r}+\beta^2\left[\frac{\omega_0^2}{(\beta v_0-\omega)^2}-1\right]\varphi=0. \quad (26)$$

The solution of this is a first-order Bessel function, so that the variation of φ with radius is as

$$J_0\left\{\beta\left[\frac{\omega_0^2}{(\beta v_0-\omega)^2}-1\right]^{\frac{1}{2}}r\right\}. \quad (27)$$

Now, suppose that the flow takes place in a metal tube of radius r_0, so that the potential must be zero at $r=r_0$. Then

$$\beta\left[\frac{\omega_0^2}{(\beta v_0-\omega)^2}-1\right]^{\frac{1}{2}}r_0=2.4. \quad (28)$$

The 4 roots of (28) will determine the values of β for any frequency ω.

We will note that the simple character of the waves has changed. The frequency of oscillation as observed moving with the flow is no longer ω_0. Although current is small for some waves and charge for others, we no longer have waves with zero current or with zero charge.

The writer will here assume baldly that the limiting current is in this case that for which

[6] C. E. Fay, A. L. Samuel, and W. Shockley, Bell Sys. Tech. J. 17, 49–79 (1939).
[7] F. B. Llewellyn and L. C. Peterson, Proc. I.R.E. 32, 144–166 (1944).

$\omega=0$. For this case we can see that for $\varphi=0$ at the tube walls,

$$(\omega_0/v_0)^2-\beta^2=(2.4/r_0)^2. \tag{29}$$

This gives only two values of β.

Looking at (2f) and (3f), we see that when $\omega=0$, v and ρ are zero when φ is zero.

Assume the conducting tube of radius r_0 has a length L and has grids covering each end, we must have $\varphi=0$ at $x=0$ and at $x=L$. Thus we must have

$$\beta L=n\pi. \tag{30}$$

Here n is an integer. From (29) and (28), the critical value of ω_0, which gives $\omega=0$, is seen to be

$$\omega_0^2=\left(\frac{2.4v_0}{r_0}\right)^2\left[1+\left(\frac{n\pi r_0}{2.4L}\right)^2\right]. \tag{31}$$

The smallest value of ω_0 for which ω can be zero is obviously that for $n=1$. Taking this value, and assuming that it represents the limiting current (not current density) I_0, we obtain

$$I_0=2^{\frac{1}{2}}2.4^2\pi\eta^{\frac{1}{2}}\epsilon V_0^{\frac{3}{2}}\left[1+\left(\frac{\pi r_0}{2.4L}\right)^2\right]$$

$$=190\times10^{-6}V_0^{\frac{3}{2}}\left[1+\left(1.31\frac{r_0}{L}\right)^2\right]. \tag{32}$$

Calbick has worked out the limiting current for an infinitely long tube in the absence of positive ions.[8] The value he obtained is

$$I_m=29.3\times10^{-6}V_0^{\frac{3}{2}}. \tag{33}$$

As might be expected, the limiting current in the presence of ions is greater than that in the absence of ions.

5. SUMMARY

In summarizing the results obtained we will first consider flow in the absence of a magnetic field or other restraining force on the electrons. In this case two types of field are possible in a space occupied by equal average charges of heavy ions and electrons. In one type the charge density is zero and the potential is one which could exist in the absence of charges. The other "wave" type of solution has an arbitrary spatial distribution of potential. For an observer having no average velocity with respect to the electrons, waves made up from the wave solution have plasma frequency. They have zero group velocity and carry no energy. There is zero current associated with them; the displacement and convection currents cancel.

When the electrons are passing the observer, the current associated with the wave solutions is still zero, but the group velocity is the velocity of the electrons and the waves can carry energy by virtue of the electrons' motion.

The wave solutions affect circuits through the intervention of other fields, in passing between grids, or through association with the other type of field in satisfying boundary conditions.

The one-dimensional case of a uniform electron current injected perpendicular to two parallel grids which are connected by zero impedance has been treated. For values of injected current below a certain critical value, depending on velocity of injection and spacing, disturbances in the stream will decay with time. For currents above this value, there will be disturbances which increase with time. Hence, this current may be regarded as the limiting current which can be transmitted through a short-circuited diode in the presence of positive ions.* This current is greater than that which can be transmitted in the absence of positive ions. In any case, the current which can be transmitted may be lowered if the diode plates are joined by an impedance other than zero.

The analysis, although based on ions of infinite mass, should not be seriously in error for ions actually encountered, at least as far as the limiting current is concerned.

Efforts to extend the analysis to cases with plane or axial symmetry have so far failed because of inability to find enough arbitrary constants to satisfy the boundary conditions.

In case the electrons cannot move perpendicular to the direction of flow (as in the case of an infinite magnetic field parallel to the flow) the boundary conditions can be satisfied. The solutions are of a mixed type. The frequency ob-

[8] C. J. Calbick, Bull. Am. Phys. Soc. 19, No. 2 (April 29, 1944).

* There is, of course, some possibility of a lower limiting current for a distribution satisfying boundary conditions over the diode grids but varying within the diode in a direction parallel to the grids.

served when moving with the flow is no longer plasma frequency. There are no zero-current or zero-charge solutions. For this type of motion, the limiting current for a conducting tube capped by grids and filled with flow has been found. It is higher than the limiting current in the absence of ions, which has been given by Calbick.

A numerical example for this last case is instructive. Assuming that the electron velocity is that corresponding to 20 volts, the limiting current in the presence of ions is approximately 0.017 ampere. This might make one expect that under many conditions the discharge in a gas tube cannot be homogeneous. Some work done by Dr. L. A. MacColl and the writer shows that in the presence of ions there are in some cases parallel plane solutions similar to those in the absence of ions,[6] but in which the potential and velocity vary periodically with distance.† These may provide a type of flow allowing a higher stable current than does the homogeneous case.

The writer wishes to express his thanks to Dr. L. A. MacColl for his generous assistance in straightening out this paper.

† *Note added in proof:* W. O. Schumann [Zeits. f. Physik **42**, 629–646 (1943)] apparently treats these solutions.

Letter to the Editor

Stereoscopy with the Electron Microscope

L. MARTON
Division of Electron Optics, Stanford University, Stanford University, California
July 24, 1944

IN a recent paper by Heidenreich and Matheson[1] a stereoscopic specimen holder (cartridge) for commercial electron microscopes is described, giving a stereo angle of 10°. The same paper ends with the following lines:

"The provision of more convenient and more precise attachments on the electron microscope for the production of stereo micrographs, such as a universal stage allowing tilting of the object to any desired angle by external control, would greatly simplify the stereo technique and eliminate the necessity of building special cartridges."

Such an universal stage was recently described by me at the January, 1944 meeting of the Electron Microscope Society. As the Heidenreich and Matheson paper does not contain any reference to my report, a brief description of this stage independent of the description of the Stanford microscope seems to be indicated.

The stage, consisting of a square piece of brass, is suspended from above on four relatively stiff brass wire rods. The suspension is held by means of two brackets, hinged around bearing surfaces, which have their axes of rotation aligned with the position of the specimen. A forked arm reaching out towards one of the pumping manifolds of the microscope and hinged on the upper part of the bracket can be moved by means of an eccentric shaft. The shaft can be rotated by means of a handle placed on the outside of the pumping manifold and made vacuum tight by means of the so-called Wilson seal. Thus the tilting of the stage can be achieved at any time by means of an external control. By tilting the bracket the stage can be tilted as much as $\pm 15\frac{1}{2}°$. The specimen holder fits into the stage by means of a tapered joint. This holder is suspended on the inserting mechanism by means of a fine hinge, thus allowing the specimen to be tilted within the same limits as the stage is tilting.

When the stage is tilted, the stage movement in horizontal directions has to be released. This cross movement

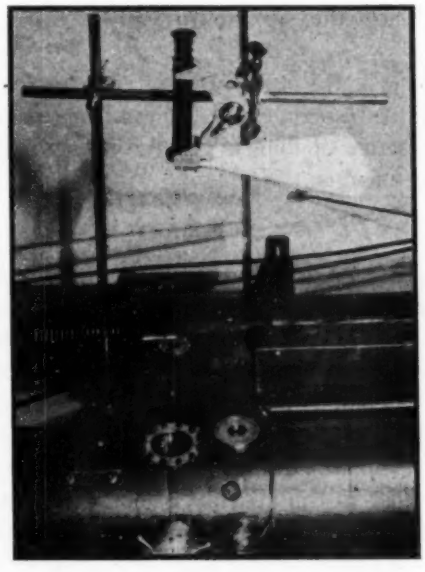

FIG. 1.

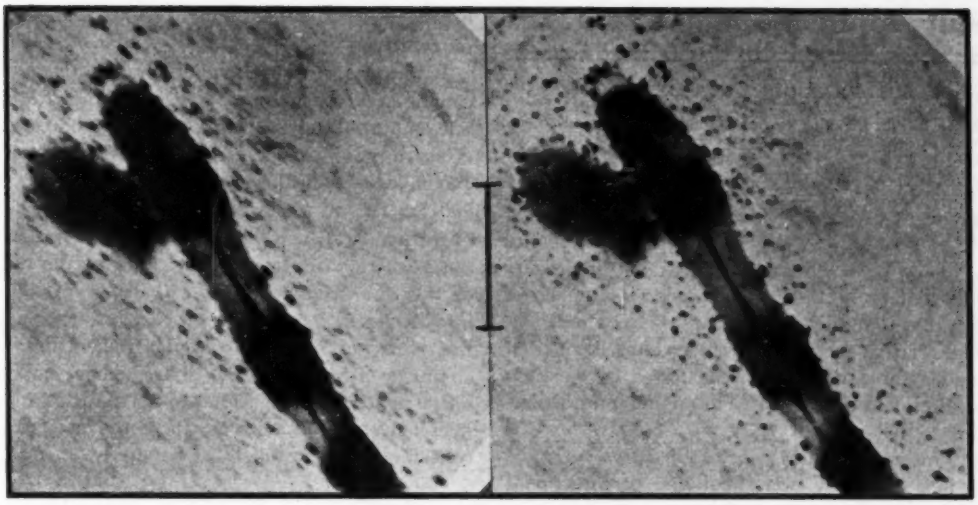

FIG. 2. Stereo micrograph of bacterial cell. Stereo angle ±10°. (Specimen, courtesy of Professor E. W. Schultz, Stanford University.)

of the stage is operated by means of a hydraulic system pressing with conveniently shaped shoes on the four sides of the stage. Two of the shoes are pointed with the shoes fitting into suitable holes on the sides normal to the tilting axis. The two other sides of the stage are cylindrical, the radius of curvature being equal to the distance from the tilting axis. The corresponding shoes are curved in a similar way. For purposes of tilting the stage the two latter shoes are withdrawn from contact with the stage by expanding corresponding parts of the hydraulic circuit. After the stage is tilted to the desired amount, the shoes are re-established in their original position.

Measurement of the tilting angle is achieved by a simple optical arrangement outside of the microscope vacuum. A small telescope, provided with a cross wire and a long index arm, views the upper part of the stage bracket which is visible through a side port of the object chamber. When the stage is tilted the telescope is rotated in its mount to align the cross wire with the visible edge of the bracket. The angle or the sine of the angle can be read on the scale attached to the telescope mount (Fig. 1).

As an example of observation at large viewing angles, bacteria are shown in Fig. 2. The internal details, made visible by this type of observation, are entirely lost at smaller stereo angles.

Further details of the Stanford electron microscope will be published in a separate paper.

[1] R. D. Heidenreich and L. A. Matheson, J. App. Phys. 15, 423–435 (1944).

Calendar of Meetings

October

5– 6 American Institute of Mining and Metallurgical Engineers. Pittsburgh, Pennsylvania
5– 7 National Electronics Conference, Chicago, Illinois
5– 7 Society of Automotive Engineers, Los Angeles, California
6– 9 Electronic Parts and Equipment Industry Conference, Chicago, Illinois
9–14 American Society of Civil Engineers, Cleveland, Ohio
10 Physics Club of Chicago, Chicago, Illinois
16–18 American Institute of Mining and Metallurgical Engineers, Cleveland, Ohio
16–20 American Society for Metals, Cleveland, Ohio
16–21 American Welding Society, Cleveland, Ohio
20–21 Optical Society of America, Hotel Pennsylvania, New York, New York
28 American Mathematical Society, New York, New York

November

2– 3 Society of Automotive Engineers, Tulsa, Oklahoma
14 Physics Club of Chicago, Chicago, Illinois
16–18 Electron Microscope Society, Chicago, Illinois
17–18 Society of Rheology, New York, New York

December

12 Physics Club of Chicago, Chicago, Illinois

January

9 Physics Club of Chicago, Chicago, Illinois

February

13 Physics Club of Chicago, Chicago, Illinois

March

13 Physics Club of Chicago, Chicago, Illinois

April

10 Physics Club of Chicago, Chicago, Illinois

May

8 Physics Club of Chicago, Chicago, Illinois

Recent Applications of Physics

Prepared by CLARK GOODMAN, Associate Editor

Material to be included in this section should be submitted to Dr. Clark Goodman, Massachusetts Institute of Technology, Cambridge 39, Massachusetts.

Communication for Trains

In applying radio and other electronic signaling principles as a means of increasing efficiency and safety in the railroad field, a number of practical train communicating methods have been developed. The relative merits of these systems have been reviewed under three general classifications by William S. Halstead, President of Halstead Traffic Communications Corporation.[1]

"(1) *Space radio systems*, in which radio wave energy is propagated into space by non-directional or directional antenna systems.

"(2) *Rail carrier telephone systems*, in which carrier signals, at frequencies usually below 10 kc, are applied primarily to the rails. Reception on mobile units is ordinarily by an inductive method, with pick-up coils located in proximity to the rails.

"(3) *Induction radio systems*, which utilize the combined induction and radiation fields generated by radiofrequency carrier-signal energy impressed on wayside conductors, such as electric power, telephone, or telegraph wires. Carrier-signal energy may be inductively impressed on wayside conductors by loop antennas installed in mobile units, or by use of inductive or capacitive line-coupling methods at fixed stations.

"Space radio systems, by virtue of their inherent ability to operate without the use of wayside wires or other conductors extending along railroad right of ways, provide the most flexible and versatile means of train communications."

However, the use of space radio presents a serious problem in that the portions of the radiofrequency spectrum where existing commercial equipment may be operated are already overcrowded. Also, because of the long distances over which a single railway system may operate, allocations of frequencies for railroad use cannot be made on a limited-area basis as is the case in the majority of the present radio installations. Studies are being made by the F.C.C. and other governmental agencies. The most likely band of frequencies lies above 300 Mc.

In rail carrier telephone communication systems there is so little radiation that Federal licensing is not required. Also a degree of privacy exists which is not ordinarily obtainable with space radio systems. Carrier-signal energy is supplied to the rails by direct metallic connection between the output circuit of the transmitter and the rails, usually by means of a connection to the insulated trucks of the locomotive or caboose. Good electrical connection between the rails is required. Because of the rapid attenuation of the carrier-signal energy, the transmitting equipment is of relatively large power output as compared with space radio apparatus. In the case of rail breakage or actual derailment the system may be rendered inoperative.

If wayside wires are available induction radio signaling can be used. Because the low impedance rail circuits are not employed, low power equipment, comparable to that of space radio, can be utilized over distances up to about 100 miles. At the low frequencies employed, from 50 to 200 kc, federal licensing is not required providing such operation is in compliance with F.C.C. regulations. In areas where wires leave the vicinity of the railroad right of way for distances greater than several hundred feet, installations of one or two wires across the gap will carry the r-f carrier signals to the point where the normal wire circuits continue. The use of frequency modulation provides relatively high signal-to-noise ratios in electric or Diesel-electric locomotives where the noise levels are of considerable magnitude.

[1] W. S. Halstead, Electronics **17**, 102 (1944).

Conducting Rubber

Those who have worn rubber-soled shoes on a dry day are well acquainted with the rather large electrostatic charge that can be built up and the sharp sparks that result when reaching for a doorknob or other grounded metallic object. This effect is obviously of practical importance for munition workers, refinery operators, and others working with explosive materials. The charges built up by automobile, bus, and airplane tires are also sometimes hazardous. The use of semiconducting rubber is the most direct solution to this problem. Acetylene or natural gas carbon blacks can be used for this purpose without sacrificing other desirable physical properties. Because of the shortage of these types of carbon black, it has become desirable to find substitutes. Special forms of channel carbon black have been developed and tested both in the natural and synthetic rubbers.[1]

It has been shown that in a typical tread stock, conductivity depends primarily on crystal structure, particle size, and surface structure of the carbon black. Of these, crystal structure and particle size are the more important properties. Recent investigations have shown that the crystal structure for most channel carbon blacks is very similar. Hence the principal factor in determining conductivity is particle size. In natural rubber, reclaim, Buna-S, Thiokol N, Neoprene GN, and Butyl (GR-I) stocks, the logarithm of the electrical conductivity is found to increase linearly as the particle size of the channel carbon black decreases from about 35 down to 10 millimicrons. The use of these fine-particle channel blacks causes a decrease in elasticity and harder processing than may be obtained with the standard channel blacks. The fine blacks also tend to retard cure. However, preliminary studies indicate that an increase in stearic acid content and in the amount of accelerator used improves the physical properties of rubber tread stocks containing fine-particle channel blacks.

[1] L. H. Cohan and M. Steinberg, Ind. Eng. Chem. **36**, 7–15 (1944).

Now Available . . .

from "High-Vacuum Headquarters"

A NEW VACUUM COATING UNIT

MODEL LC1-500-3

THIS important new DPI unit is intended for the application of low-reflection coatings, or the depositing of metals such as silver, gold, aluminum, etc.—or metallic salts—on glass, metal, crystalline materials, and plastics.

FEATURES

1. *Automatic bell-jar lift* Promotes ease of operation.

2. *High-vacuum valve* An optional feature which enables the diffusion pump to run continuously.

3. *Fast evacuation cycle* Less than two minutes. If very fast evacuation cycle is necessary, a large roughing pump can be incorporated, making pressures of 0.0001 mm. Hg. possible in less than two minutes.

4. *Rugged construction* Unit is designed and built for production work, without sacrificing appearance.

5. *Low maintenance* Not much that can "go wrong." In case of trouble, machine can be serviced easily.

6. *Simplicity* Location of valves, gauges, switches makes for easy operation. Because of construction features, machine is easy to keep clean.

7. *Completeness* Unit comes ready for operation. Includes high-speed diffusion pump, mechanical pump, forepressure gauge, Pirani and Ionization gauges to read pressures in bell jar, thermocouple gauge to read temperatures in bell jar, heater and filament gauges and controls, pneumatic bell-jar lift, wiring and other service connections.

Write to DPI—*Vacuum Equipment Division*—for further details about this coating unit, or for information on complete vacuum systems to suit other needs.

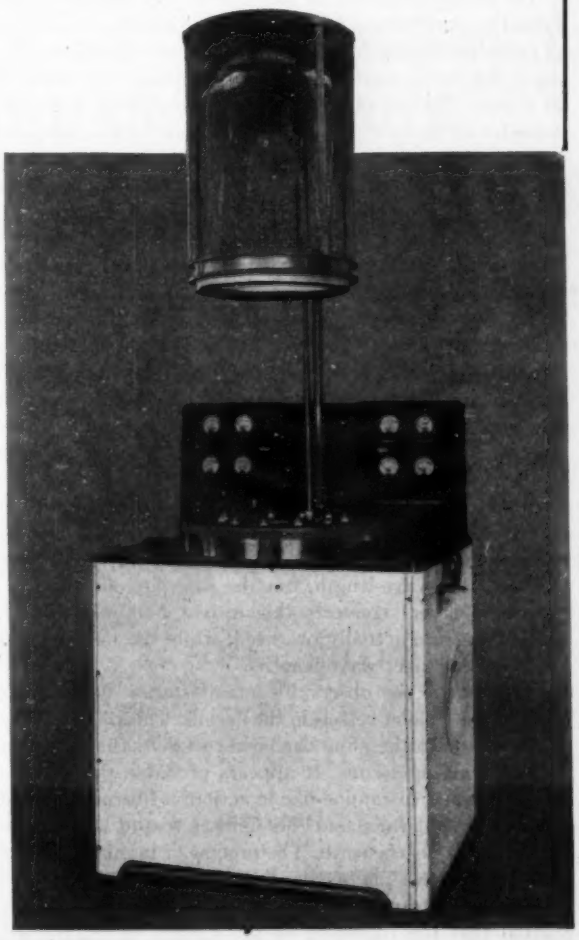

DP INC. HIGH-VACUUM HEADQUARTERS

DISTILLATION PRODUCTS, INC.

VACUUM EQUIPMENT DIVISION

ROCHESTER 13, N. Y.

U. V. and You Although the photophysiologic processes which cause sunburn are not thoroughly understood, considerable progress has been made through absorption and action spectra studies.[1] Proteins and nucleic acids, present in the epidermis, strongly absorb at wave-lengths below 3200A. This region comprises a tiny fraction of sunlight but is well represented in the emission of the common intermediate pressure (therapeutic) mercury arc. Sunlight penetrates only a short distance into the skin, the maximal occurring at about 7500A, i.e., in the infra-red just beyond the visible region. Such radiation is reduced to 1 percent of its incident intensity after penetrating a few millimeters. Wave-lengths shorter than 3200A, on the other hand, do not penetrate more than 0.1 mm. However, within this depth, changes are produced that seem comparable to lethal and injurious effects on unicellular organisms. The grossly observable changes are a series of events including erythema and suntan.

The action spectrum for the erythema of sunburn is obtained by determining for various wave-lengths the amount of radiation required to produce a just perceptible reddening of the skin at a given time after its application—usually 24 hours. The rate of development of erythema is not the same for all wave-lengths, and since this is not considered in evaluating such observations, there is some question whether the action spectrum so obtained is an accurate index of the photochemical reaction in the skin. However, the general character of the action spectrum reflects the absorption spectrum of the substance (probably protein or nucleic acid) primarily affected by the radiation. This absorption sets the long wave-length limit at about 3200A, as mentioned above. The shape of the action spectrum is greatly affected by the superficial horny layer, not itself involved in the erythema process, which acts as an effective screen to cut off ultraviolet radiations of these wave-lengths. A minimum is displayed by the action spectrum at about 2800A, which corresponds to a maximum of absorption of the epidermis and also to a maximum of absorption for typical protein. The primary photochemical process underlying the erythema probably has its maximum at about this wave-length, but the screening effect of the superficial layers converts this into a minimum in the action spectrum actually observed, while the maximum is displayed to longer wave-lengths.

Erythema is the observable manifestation of dilations of the minute blood vessels in the dermis. This dilation may be secondary to the photochemical reactions that occur in the overlying epidermis. It appears probable that a dilatory substance, histamine-like in action, is liberated by the cells of the epidermis, and this diffuses to and acts on the blood vessels just beneath. The process of tanning appears to consist of two major changes. The first phase follows erythema, the transition from red to brown color being so gradual that the transition of tan cannot be determined accurately. This first phase of tanning is a consequence of the same photochemical changes that lead to erythema, although the exact relationship between the two phenomena is not clearly understood. Both have the same action spectrum and both may be expressions of changes in the epidermis that are similar to the destructive effects generally produced in cells by radiation shorter than 3200A. Another component of tanning is observed only in skins that already show a certain degree of suntan. It begins immediately upon exposure to sunlight, before erythema appears; and its rate of development bears no direct relationship to the latter. Moreover, the action spectrum of this second phase of tanning is very different from that erythema, demonstrating that the two processes are initiated by different photochemical mechanisms.

The second phase is induced by wave-lengths between 3000 and 4000A, and requires several hundred times the intensity of radiation which produces erythema. Moreover, the second phase of tanning requires the participation of oxygen derived from the blood. With exposure to the mercury arc, much of the radiation is within the action spectrum of erythema and the first phase of tan, but relatively little within the action spectrum of the second phase. Hence, tanning produced by the mercury arc is usually much less intense than that produced by sunlight sufficient to cause a light degree of erythema. Melanin pigment appears to be the most important factor in tanning, but reduced hemoglobin may contribute in the early stages. The second phase of tanning appears to result from the oxidation of melanin pigment already in the skin in a colorless form.

[1] H. F. Blum, *Medical Physics* (The Year Book Publishers Inc., Chicago, 1944), pp. 1145–1157.

Physics Applied to Aviation Physiology The marked improvement in plane performance in the last few years has increased the demands upon the pilot to the point where he has become the limiting factor in flight. The extreme linear and radial accelerations and the decrease in atmospheric pressure with altitude are of predominant importance. Two recent reviews of the subject[1,2] are not only of interest to practical-minded physicists but offer a challenge to them to devise methods of counteracting these effects.

Linear accelerations of considerable magnitude are experienced during catapult take-offs, crash landings, and parachute jumps. With ordinary take-offs, the acceleration in the anteroposterior axis of the body rarely exceeds 0.2 to 0.5 g, but with catapult launchings this may be increased to between 2 to 4.5 g for 0.8 to 1.5 seconds. However, accelerations up to 17 g in the transverse axis may be endured without serious trouble. Hence, such catapult take-offs cause no difficulty provided the pilot's head and body are well-pressed against the seat pillows at the start. In normal landings the accelerations are only a fraction of 1 g. In pancake landings this may be increased to 4½ g; while crashing of the plane against a fixed object in which the plane collapses and the pilot's body comes to a stop in about a yard, may increase the acceleration forces to 45 g and higher. If the pilot is properly strapped in place, he may escape injury even in the latter type of accident. On jumping from an airplane, the pilot is accelerated until the wind resistance equals the force of gravity, after which he falls at a constant terminal velocity of between 150 and 200 ft. per second. Without a parachute, he would be

"Photographic Plates for Use in Spectroscopy and Astronomy"

FIFTH EDITION

A ***new, fully revised edition*** of this well-known publication is available. In it are listed the characteristics of the special plates for scientific work which are made in the Kodak Research Laboratories. There are over one hundred kinds of these plates, distributed among seven basic types of emulsion, each carefully prepared to provide desirable combinations of speed, contrast, granularity, and resolving power. They are sensitized in various ways to permit photography in spectral regions ranging from the short-wave-length ultraviolet to the infrared at 12,000Å.

A copy of the new edition of the booklet will be sent free upon request.

EASTMAN KODAK COMPANY

Research Laboratories **Rochester 4, N. Y.**

GAERTNER

Instruments for Spectrographic Analysis

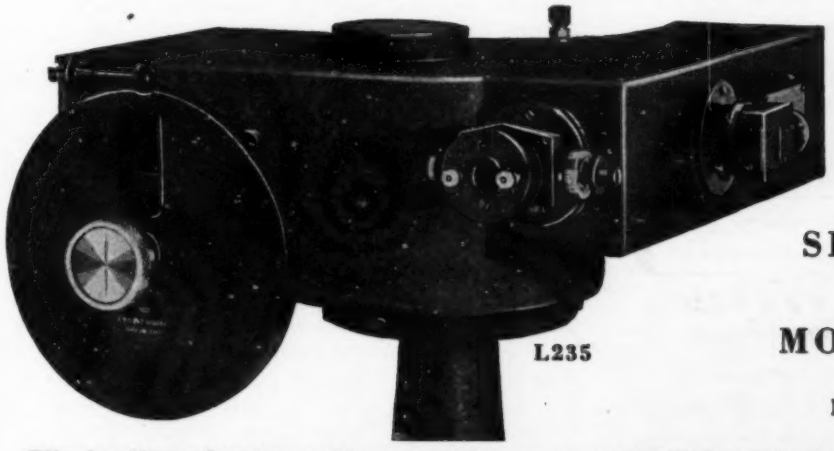

L235

INFRA-RED

SPECTROMETER and MONOCHROMATOR

Range: 0.7μ to 12.0μ

Elimination of Astigmatism and Coma • High Transmission • Extreme Accuracy

together with the skillful design and workmanship incorporated in this instrument render it exceptionally well-fitted for exacting research work.

THE GAERTNER SCIENTIFIC CORPORATION

1212 WRIGHTWOOD AVE. • CHICAGO 14 • U.S.A.

PHOTO COURTESY OF FOXBORO COMPANY

PROFITABLE volume production in the heat treating and chemical industries depends on accurate, automatic control. Potentiometers provide this vital factor if equipped with dependable standard cells, thus protecting your profits.

For a quarter century the great majority of Potentiometers have depended on EPLAB standard cells for accuracy. These cells act as a "yardstick" for translating voltage to temperature or pH. The first commercial cells of their type in America and constantly improved by research, they are today "as standard as sterling".

SPECIFY EPLAB CELLS when you order Potentiometric Instruments

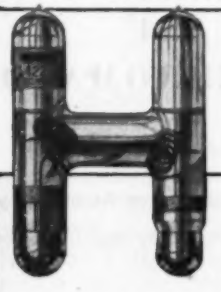

THE EPPLEY LABORATORY, INC.
Scientific Instruments
Newport, R. I., U. S. A.

EPLAB
STANDARD
CELLS
"As Standard as Sterling"

Recent Applications of Physics (continued)

decelerated by the ground at between 360 and 720 g in a distance of 1 to 2 ft. If the parachute is opened after the terminal velocity has been reached, the pilot slows to a speed of approximately 20 ft. per second in a distance of about 90 ft. This deceleration is equivalent to between 5 and 6 g, giving a total of 6 to 7 g acting against the seat and pelvic regions for about one second.

Most combat planes travel with speeds greater than the terminal velocity of a freely falling body; and if the pilot pulls his rip cord immediately upon leaving the plane, his deceleration may be as great as 10 to 14 g. For this reason, the rip cords on parachutes for use on fast planes are of the manual-operated rather than the anchored type in order to allow sufficient time for the wind resistance to reduce the initial speed of the pilot's body to the terminal velocity before he opens his parachute. If the pilot bends his hips and knees smoothly, the shock of striking the ground at the end of a parachute jump may amount to only 2.5 g, which added to the gravitational pull gives a total force of about 3.5 g or the equivalent of that experienced in jumping from a 10-ft. height.

Effects of radial accelerations have been studied in actual flights and in large centrifuges. At a total of 2 g the pilot notices only increased pressure on the feet or seat. At 3 to 4 g difficulty is experienced in standing, the muscles are reflexly tensed, respiration is increased, and the soft tissues of the face are drawn downward. At 5 g the body becomes immovable, standing is impossible, and respiration is stopped in mid-inspiratory as a defense against the dragging sensation in the thorax. Between 5 and 9 g the legs become congested, the calf muscles cramp, vision is lost (blacking out), sharpness of hearing is decreased, reaction time is increased, and finally, in most individuals loss of consciousness occurs. The blacking-out and unconsciousness are due to cessation of the blood flow caused by a decline in the arterial pressure. At a radial acceleration of 7.8 g the blood virtually becomes as heavy as molten iron. Assuming that the heart can maintain a normal pressure at the aortic arch of 120 mm Hg (160 cm of water) during an acceleration of 5 g, then at a point 30 cm above the aortic arch, that is, at the base of the skull, the pressure would be reduced from the normal of 130 cm of water to 10 cm of water ($160-5\times30=10$). The brain and eyes can only function for a few seconds without their normal blood supply, and loss of vision and blacking-out is due to the failure of the circulation in the retina of the eye. If the acceleration is maintained, the blood supply of the brain fails and the pilot becomes unconscious. The best method for increasing tolerance to radial acceleration in flight is to place the pilot with his face down on the floor of the plane or to provide for rotating his seat so that he is supine during the pull-out. Either of these converts the acceleration force from the longitudinal to the transverse axis of the pilot. No disturbances of vision or of sensation are seen until the transverse accelerations exceed about 12 g. Unfortunately, these positions may interfere with the vision, and hence may not be of practical application.

[1] H. D. Green, *Medical Physics* (The Year Book Publishers Inc., Chicago, 1944), pp. 22–26.
[2] B. H. C. Mathews, Nature **153**, 698–702 (1944).